

Distribution Agreement

In presenting this thesis as a partial fulfillment of the requirements for a degree from Emory University, I hereby grant to Emory University and its agents the non-exclusive license to archive, make accessible, and display my thesis in whole or in part in all forms of media, now or hereafter now, including display on the World Wide Web. I understand that I may select some access restrictions as part of the online submission of this thesis. I retain all ownership rights to the copyright of the thesis. I also retain the right to use in future works (such as articles or books) all or part of this thesis.

Brittany File

March 27, 2017

Characterization of the Immune Environment in the Post-Mortem Spinal Cord Tissue of ALS
Patients and Controls

by

Brittany File

Jonathan Glass, M.D.
Adviser

Department of Neuroscience and Behavioral Biology

Jonathan Glass, M.D.
Adviser

Marla Gearing, PhD
Committee Member

Leah Roesch, PhD
Committee Member

Patrick Cafferty, PhD
Committee Member

2017

Characterization of the Immune Environment in the Post-Mortem Spinal Cord Tissue of ALS
Patients and Controls

By

Brittany File

Jonathan Glass, M.D.

Adviser

An abstract of
a thesis submitted to the Faculty of Emory College of Arts and Sciences
of Emory University in partial fulfillment
of the requirements of the degree of
Bachelor of Sciences with Honors

Department of Neuroscience and Behavioral Biology

2017

Abstract

Characterization of the Immune Environment in the Post-Mortem Spinal Cord Tissue of ALS Patients and Controls

By Brittany File

Amyotrophic lateral sclerosis (ALS) is a neurodegenerative disease that causes progressive muscle weakness and ultimately death due to respiratory failure. There is no cure for ALS, and its causes are unknown. Neuroinflammation is a notable pathological finding present at the site of motor neuron death in spinal cords of patients with ALS, and it is suggested that inflammation may have both protective and deleterious effects on neuronal survival. Microglia are innate immune cells that function as actors in immune surveillance of the central nervous system (CNS) and can become active contributors to neuroinflammation. With activation, microglia undergo morphological changes that are recognized during neuropathological evaluation. While it is hypothesized that the immune system first responds to aid and repair damaged motor neurons, it has also been suggested that as ALS progresses the once neuroprotective response shifts to a self-sustaining cycle of neurotoxicity and cell death. This project extends such research and investigates the presence of inflammatory markers, specifically microglia, in spinal cords collected at autopsy from patients dying with ALS. In addition, we investigated the possible effect on microglial reactivity in patients that participated in a clinical trial of intraspinal transplantation of stem cells for ALS. The aims of this study are two-fold: 1) to compare microglial activation in the spinal cords of ALS patients versus age-matched disease and normal (no neurological disease) controls; and 2) to determine whether the injection of neural stem cells alters the local immune environment in post-mortem tissue of the ALS patients.

Characterization of the Immune Environment in the Post-Mortem Spinal Cord Tissue of ALS
Patients and Controls

By

Brittany File

Jonathan Glass, M.D.

Adviser

A thesis submitted to the Faculty of Emory College of Arts and Sciences
of Emory University in partial fulfillment
of the requirements of the degree of
Bachelor of Sciences with Honors

Department of Neuroscience and Behavioral Biology

2017

Acknowledgements

I would first like to thank David Gutman, M.D./PhD for his continuous support throughout this project and assistance in the creation of the technology and programming that made this project possible.

I would also like to thank Mfon Umoh, Tezeta Tadesse, and Seneshaw Asress, PhD, members of the Glass laboratory for helping me when I first joined the laboratory. It was with their initial encouragement and guidance that I am now able to bring this project to completion.

I also thank Marla Gearing, PhD, for her endless support and patience during the ups and downs of this project. In helping direct me in everything from pathological analyses to statistics, she was a critical component in my success.

I would like to thank Leah Roesch and Patrick Cafferty, PhD, for their participation on my thesis committee. I have learned so much from their classes and they have helped me in taking my scientific skills to the next level.

My final thanks is reserved for Jonathan Glass, M.D., my mentor and principal investigator. Dr. Glass has been an extremely influential person in my growth as a student, researcher, and person. His endless curiosity and pursuit for knowledge has truly inspired me to continue my own journey in the scientific world.

Table of Contents

1. Abstract.....	1
2. Introduction.....	2
3. Materials and Methods.....	9
4. Results.....	13
5. Discussion.....	22
6. Limitations and Future Directions.....	27
7. Figures & Tables.....	29
Table 1. Disease characteristics for the four subject groups.....	29
Figure 1. Differences in density of microglial populations noted between medial and lateral anterior horn.....	30
Figure 2. Annotating the region of interest (anterior horn) in Aperio ImageScope.....	31
Figure 3. Quantitative analysis of microglia using the object counts.....	32
Figure 4. Quantitative analysis of microglia using the object area.....	32
Figure 5. Quantitative analysis of microglia using positive pixel count.....	33
Figure 6. Qualitative analysis of microglial populations in control spinal cords.....	34
Figure 7. Qualitative analysis of microglial populations in ALS spinal cord.....	34
Table 2. A summary table of an initial analysis of non-disease control vs ALS spinal cords.....	35
Figure 8. Microglial population analyses within varying region in non-disease control spinal cord.....	36
Figure 9. Microglial analyses of the rostral spinal cord in non-disease control, disease control, and ALS patients.....	37

Figure 10. Analysis of microglia area in the rostral spinal cord in non-disease control and ALS patients.....	38
Figure 11. Microglial population analyses of the caudal spinal cord in non-disease control, disease control, and ALS patients.....	39
Figure 12. Microglial population analyses of the caudal spinal cord in non-disease control and ALS patients.....	40
Figure 13. A comparison of injected and non-injection spinal cord regions in case 5.....	41
Figure 14. Stem cell treated sections of spinal cord exhibit regions of clearing.....	42
Table 3. A summary table of an initial analysis of stem cell positive vs negative regions.....	43
Figure 15. Microglial population analyses of stem cell positive vs negative regions.....	44
Figure 16. Correlation analyses within stem cell positive regions.....	45
Table 4. Quantitative analysis results for individual non-disease control, control, and ALS cases.....	46
Table 5. Quantitative analysis results for individual stem cell cases.....	47
8. References	48

Abstract

Amyotrophic lateral sclerosis (ALS) is a neurodegenerative disease that causes progressive muscle weakness and ultimately death due to respiratory failure. There is no cure for ALS, and its causes are unknown. Neuroinflammation is a notable pathological finding present at the site of motor neuron death in spinal cords of patients with ALS, and it is suggested that inflammation may have both protective and deleterious effects on neuronal survival. Microglia are innate immune cells that function as actors in immune surveillance of the central nervous system (CNS) and can become active contributors to neuroinflammation. With activation, microglia undergo morphological changes that are recognized during neuropathological evaluation. While it is hypothesized that the immune system first responds to aid and repair damaged motor neurons, it has also been suggested that as ALS progresses the once neuroprotective response shifts to a self-sustaining cycle of neurotoxicity and cell death. This project extends such research and investigates the presence of inflammatory markers, specifically microglia, in spinal cords collected at autopsy from patients dying with ALS. In addition, we investigated the possible effect on microglial reactivity in patients that participated in a clinical trial of intraspinal transplantation of stem cells for ALS. The aims of this study are two-fold: 1) to compare microglial activation in the spinal cords of ALS patients versus age-matched disease and normal (no neurological disease) controls; and 2) to determine whether the injection of neural stem cells alters the local immune environment in post-mortem tissue of the ALS patients.

Background

Amyotrophic Lateral Sclerosis

Amyotrophic Lateral Sclerosis (ALS), also known as Lou Gehrig's disease, is a progressive neurodegenerative disease estimated to affect 1-2 per 100,000 people per year with a five-year survival rate of only 7% (del Aguila, 2003; McGuire, 1996). ALS is characterized by the progressive loss of upper and lower motor neurons, which manifests in symptoms of muscle weakness, fasciculations (twitching), and cramping, and eventually results in a complete loss of voluntary movement. In the late stages of ALS patients develop symptoms of dyspnea due to denervation of the respiratory muscles, which ultimately leads to death (Chio, 2009). Males appear to have an increased risk of developing the disease compared to women with a relative risk of 1.6:1. The median age of onset is about 55 years (Manjalay, 2010; Pasinelli, 2006). ALS can be classified into two distinct categories, with the majority falling under sporadic ALS and 10% of cases classified as inherited, or familial, ALS (Chen, 2013). Under both of these classifications, dysfunction of upper and lower motor neurons causes deterioration and death of motor neurons, which ultimately severs the link between the nervous system and the body's voluntary muscles while sparing the sensory systems and oculomotor control (Appel, 2011).

Regions of Onset

Symptoms of ALS present regionally within the lower limb, upper limb, or bulbar musculature. ALS patient's typically first experience localized asymmetric muscle weakness that progresses to include both upper motor neuron and lower motor neuron signs of degeneration affecting bulbar, cervical, thoracic, and lumbar areas (Gordon, 2006; Zarei, 2015). This degeneration eventually leads to respiratory failure and/or total voluntary muscle paralysis.

Bulbar onset is typically associated with a worse prognosis compared to upper or lower limb onset (del Aguila, 2003; Louwse, 1997). Similarly, ALS patients with isolated respiratory onset symptoms, although rare, have a particularly poor prognosis, as respiratory failure is a common cause of death in ALS (de Carvalho, 1996). Improving the understanding of the pathogenesis of ALS is critical to the development of new diagnostic techniques and treatments for the disease as there is only one FDA approved drug treatment for ALS that prolongs survival by approximately 10% compared to placebo (Czaplinski, 2006).

Motor Neurons and Neuroinflammation

Motor neurons in the anterior horn of the spinal cord control all voluntary muscle movement such as motor activity, respiration, speech, and swallowing functions. Morphological changes occur in the anterior horn in ALS and are characterized by loss of motor neurons and gliosis (Ghatak, 1986). The mechanism behind motor neuron loss observed in ALS is still unclear, but many mechanisms have been proposed including the unfolded protein response (ER stress), abnormal RNA/DNA regulation, glutamate excitotoxicity, mitochondrial dysfunction, oxidative stress, and glial cell pathology (Rothstein, 2009). Neuroinflammation at the site of motor neuron death in the brain and spinal cord of ALS patients is also a notable pathological finding (Lasiene, 2011). Neuroinflammation is characterized by the presence and proliferation of astrocytes, microglia, macrophages, and T-lymphocytes at the site of primary pathology (Phillips, 2011). Evidence of gliosis is noted as a typical pathological feature in the anterior horn of patients dying with ALS (Papadimitriou, 2010).

Microglia in Normal Immune Response

Microglia are resident cells of the CNS involved in the innate immune response, providing the first line of defense against threats to the sensitive environment of the brain and spinal cord. Microglia act as immune effectors as they search for foreign microorganisms or compromised cells (Moisse and Strong, 2006). In the adult brain, it is thought that microglia are also involved in the maintenance of homeostasis and regulation of the extracellular environment, as well as contributing to the neural network by aiding in synaptic remodeling and plasticity (Harry, 2013). In a normal adult brain microglia are present in a resting state, but when injury or disease is detected microglia are able to quickly activate in response to molecular signals such as cytokines and chemokines, including proinflammatory interferon- γ and tumor necrosis factor α , which originate from neurons and astrocytes (Moisse and Strong, 2006). Many theories are proposed to explain the mechanism behind microglial responsiveness including the presence of inward rectifying K^+ channels, but no outward currents, (Kettenmann, 1993), activation of adenosine triphosphate receptors (Waltz, 1993), the actions of calcitonin gene-related peptide (Priller, 1995), and activity of other neurotransmitter receptors (Pocock and Kettenmann, 2007).

Dual Role of Microglia in ALS

In the normal adult brain, it is thought that healthy neurons maintain the inactivated state of microglia via secreted and membrane bound signals such as CD200, CX3CL1, neurotransmitters, and neurotrophins (Biber, 2007). When these neurons are affected by disease or physical damage, the loss of receptor activation may alter the functional state of surrounding microglia. Microglia have the capacity to secrete cytotoxic elements such as reactive oxygen species, nitric oxide, proteases, arachidonic acid derivatives, excitatory amino acids and

cytokines; however, they also are able to produce neuroprotective effects such as phagocytosis of dead neurons and secretion of neurotrophic factors and neuroprotective cytokines (Elliot, 2001; Weydt, 2004; Liao, 2012).

A current model of how the immune system functions during the course of ALS is that it first reacts to motor neuron damage by moving to repair and regenerate the damaged tissue. However, as ALS progresses, it is thought that the once neuroprotective immune response shifts to a self-sustaining cycle of neurotoxicity and cell death. The question arises as to whether microglial activation promotes motor neuron survival or contributes to motor neuron death, or whether both functionalities may come into play with disease progression (Moisse and Strong, 2006). In an animal model of ALS using the transgenic mutant Cu-Zn superoxide dismutase (mSOD1) mouse, it was demonstrated that wild-type microglia, which secrete neurotrophic factors, free radicals, and anti-inflammatory cytokines, promote neuroprotection of motor neurons (Beers, 2006; Gurney, 1994).

The distinctly different pathological and morphological states of microglia suggest that microglia can be divided functionally into classically activated “neurotoxic” microglia (M1) and alternatively activated “neuroprotective” microglia (M2) (Zhao, 2013). The negative effect of M1 microglia, or activated glia, stems from their secretion of Reactive Oxygen Species (ROS) and proinflammatory cytokines, such as $\text{TNF}\alpha$, IL-6, IL- 1β , interferon- γ (IFN γ), and proinflammatory chemokines, which creates a cytotoxic environment promoting motor neuron death in ALS (Boche, 2013; Zhao, 2013). In contrast, M2 microglia are characterized as “neuroprotective” due to their secretion of anti-inflammatory cytokines and neurotrophic factors, such as IL-4, IL-10, YM1, ornithine, and polyamines (Martinez, 2009; Zhao, 2013). The mSOD1 transgenic mouse model of ALS was used to study the roles of M1 and M2 microglia. These

authors showed that the M2 microglia phenotype, via up-regulated M2 markers CD206 and YM1, is observed in early stage ALS while the M1 microglia phenotype, via increase levels of NOX2 and IL-1 β is observed in the rapidly progressing phase (Zhao, 2013; Beers, 2011b). This spectrum of M1-M2 microglia and the distinct phenotypic characteristics of microglia can influence the progression of ALS, but research suggests that the M1-M2 microglia paradigm may be more complex, and these physiological features of microglia may exist on more of a continuous spectrum (Henkel, 2009; Komine, 2015).

Data in humans using immunohistochemistry (IHC) and antibodies to the actin-binding protein IBA-1, an established IHC marker for microglia that identifies both resting and active microglia (Ito, 1998), suggests that microglial pathology correlates with disease progression and axonal loss in the corticospinal tract (CST), with the extent of microglial activation rated using semi-quantitative methods on an ordinal scale (0, none; 1, mild; 2, moderate; 3, severe/numerous) (Brettschneider, 2012). Furthermore, patients assessed clinically to have a higher burden of UMN disease showed a greater extent of microglial pathology in the cervical anterior horns and CST when compared to patients with less evidence of UMN disease (Brettschneider, 2012).

Targeting Microglia for Therapy in ALS

Neuroinflammation, and specifically microglia, has been a target for controlling the pathogenesis of ALS that has proved successful in ALS mouse models. Oxidative stress caused by mutations in superoxide dismutase-1 (SOD1) has been noted as a prominent factor in neurodegeneration and contributes to progressive motor neuron loss in the cerebral cortex, brain stem, and spinal cord in ALS (Rosen, 1993). The elimination of microglia-derived superoxide by

treatment with apocynin resulted in a significantly slowed disease progression in mutant SOD1 mouse model (Harrasz, 2008). Additionally, blocking excess glutamate secreted from microglia significantly slowed disease progression in the SOD1 mouse model (Takeuchi, 2011). Lastly, recent studies have demonstrated that the elimination of micro RNA (miR-155), which is elevated in human ALS and mutant SOD1 mice, extended survival time of SOD1 mice through the restoration of microglial functions and aiding in the reduction of neuroinflammation (Butovsky, 2015).

Quantification of Microglia in the Spinal Cord

In previous studies, microglia were analyzed using semi-quantitative measures with categorical ratings that encompassed morphological and immunoreactivity changes (Brettschneider, 2012; Colburn, 1977). In one study, an unbiased counting frame was created around a particular lesion and sample areas were randomly generated, quantified, and then multiplied to obtain an estimate of the total microglial number (Donnelly, 2009). This study aimed to find a simple, rapid, and sensitive method with minimal bias to assess microglia and macrophages across lesions, and resulted in an efficient and reproducible method for cell counting. In a mouse model, microglial quantification was performed on every 8th section of lumbar spinal cord (Frakes, 2014). Using this method, data provided a mechanism by which microglia induce motor neuron death by inhibiting nuclear factor-kappa B, a regulator of inflammation.

Stem Cell Transplantation as Therapy

The transplantation of stem cells into the spinal cord of ALS patients is proposed as a promising method of therapy based on the assumption that stem cells have an inherent ability to differentiate into various specialized cells. It is thought that by introducing stem cells into the spinal cord they would be able to target specific mechanisms related to the pathogenesis of ALS (Meamar, 2013). Stem cells could have the ability to replace damaged cells, create a new and supportive environment for diseased host cells, or modify the immune environment to make it more viable for cell survival. In the mSOD1 rat model of ALS, the injected stem cells differentiated into glial cells and neurons that integrated into the existing neural network (Xu, 2006). These human spinal cord-derived stem cells (HSSCs) secreted glial-derived neurotrophic factor (GDNF) and brain-derived neurotrophic factors (BDNF), which suggest that they may provide trophic benefits for motor neurons. In this experimental model, the transplanted spinal cord-derived stem cells had a positive effect on animal survival. Because of the success in the animal models, HSSC transplantation into the spinal cord is now being tested as a therapy for human ALS (Glass, 2012; Feldman, 2014; Glass, 2016). Post mortem analysis of participants in this trial identified transplanted neural stem cells in the spinal cord of ALS patients, demonstrating the ability of these cells to survive for long periods of time after transplantation, with at least partial differentiation into neuronal and glial cells (Tadesse, 2014). These tissues were used for this project, allowing us to ask whether the inflammatory milieu, as identified by microglial abundance and morphology, was affected by the transplantation of HSSCs.

Materials and Methods

Subject Groups

Spinal cord tissues were analyzed from four different subject groups: control without disease, control with disease (Alzheimer's), ALS, and ALS/stem cell injected cases. The gender, PMI, age at onset, age at death, and disease duration for all four patient populations can be seen in Table 1. Subjects were age-matched to the best of our ability.

Immunohistochemistry

Immunohistochemistry (IHC) was performed on 8 μ m paraffin-embedded sections from human post-mortem cervical, thoracic, lumbar, and sacral spinal cord tissues from non-neurological disease controls, neurological disease controls, ALS, and ALS/stem cell injected cases. Stem cell injected tissue sections were divided into two groups: sections marked positive as showing the presence of stem cells in that section, and sections marked negative as presumably being absent of stem cells. Stem cell negative sections were chosen far from the spinal cord region that received the stem cell injections and had no observable stem cell clusters. Prior to IHC, sections were subjected to antigen retrieval by microwaving in citrate buffer. Endogenous peroxidase activity was blocked with 3% hydrogen peroxide in 100% tris-buffered saline (TBS). Non-specific staining was inhibited by blocking for one hour in 10% normal goat serum in TBS +1% bovine serum albumin (BSA). Sections were then incubated overnight with a rabbit antibody to Iba1 (1:500, Wako 019-19741), a marker for human microglia. Sections were then incubated with biotinylated secondary antibody (1:1000) for one hour, followed by avidin-biotin peroxidase complex (Vector Laboratories) for one hour. The immunoreactive product was labeled using 3,3'-diaminobenzoic acid (DAB) peroxidase substrate kit (Vector Laboratories),

and counterstained with hematoxylin. Finally, slides were washed and cover-slipped. All staining procedures were performed using appropriate positive and negative controls. Staining and subsequent analyses were performed blinded to clinical diagnoses and procedures.

Initial Image Analysis

Blinded qualitative analysis of control and ALS cases was performed using microscopic images to identify the relative density of microglia populating the anterior horn. Differences in morphology, spread, and clustering of microglia were observed at a magnification of 20X. Differences within the medial (center) and lateral (lower) regions of the anterior horn were noted (Fig. 1). Representative images of the left and right anterior horn, medial and lateral regions, of non-disease control, ALS, and ALS patients who were injected with neural stem cells were taken at a magnification of 40X and analyzed using the object count function in Image Pro Premier 9.1 (Media Cybernetics, Rockville, MD). Relative amounts of microglia within the anterior horns in each section were defined on a semi-quantitative scale defined as: ≤ 20 (+), 21-31 (++), 32-42 (+++), and ≥ 43 (++++).

Object Count and Area Measure

The glass slides were scanned into a digital format using an Aperio AT2 scanner (Leica Biosystems, U.S.A.). Aperio ImageScope software was used to view the digitally scanned slides. Once in ImageScope, a stylus was used to draw a free-form annotation, or region of interest, to distinguish between the target region (anterior horn grey matter) and the non-target region (white matter) (Fig. 2). Annotated regions of interest were transferred to Image Pro Premier 9.1 for quantitative assessment of the number of microglia present in the anterior horn using the method

of object count (Fig. 3). Using the “dark objects” setting, discrete, separate objects (microglia) were identified and counted automatically using restrictive parameters for object (microglia) intensity and area. The darkness parameter was set to optimize the accuracy of the microglial count. Range settings were further utilized to set a standard for area and intensity of the objects to be counted with a lower limit set to optimize recognition of microglial cell bodies. The number of counted objects for each image was recorded and the average area of microglial cell bodies in each region of interest was measured using the masks created via Image Pro Premier (Fig. 4).

Aperio ImageScope Positive Pixel Count

The positive pixel count algorithm within Aperio ImageScope was used to quantify the amount of a specific stain present in a scanned slide image based on pre-specified color parameters. The algorithm detects pixels that match the user-specified color parameters, which are defined by positive stain color and intensity thresholds using the HSI (Hue, Saturation, Intensity) color model. Each multi-colored image is made up of red, green, blue (RGB) component values and image analysis determines the RGB pixel values of the image-stain.

Standard IHC staining protocol is designed to maximize contrast between the blue counterstain and the brown DAB stain. We leveraged existing Aperio ImageScope hue value parameters to identify positively DAB stained brown pixels. Hue width is the range of accepted positively stained pixels centered on the hue value. The larger the hue width, the larger range of “brown” accepted as positive. Due to the wide range of brown exhibited by DAB staining of microglia, from the cell body to the end of the processes, the hue width was set at the largest parameter reasonably accepted in the algorithm.

Another parameter within Aperio ImageScope to detect pixels is the intensity, which measures the brightness of the pixel and ranges from zero (black) to 255 (bright white). The positive pixel count organizes pixels into four color-masked categories depending on set intensity parameters: negative (blue), weak-positive (yellow), positive (orange), and strong-positive (red). Weak-positive pixels are identified as those that are towards the brightest range (255) and strong-positive pixels are those towards the darkest range (0). Pixels that do not meet the hue/saturation parameters, but have an intensity value less than weak-positive pixels are classified as negative pixels. Those strong positive pixels (red) identified the microglial cell body and processes most accurately (Fig. 5). A pixel score was assigned to each spinal cord region by dividing the number of strong positive pixels by the number of total pixels and subsequently multiplied by 100 to create a final number that represented the proportion of the spinal cord region occupied by microglia.

Statistical Analyses

Statistical analyses were performed using Graphpad Prism 6 software (La Jolla, CA). Data were tested for a parametric distribution using the Kolmogorov-Smirnov test ($p < .05$). Parametric data were subsequently analyzed using analysis of variance (ANOVA) when comparing more than two groups, or t-tests when comparing two groups. Furthermore, correlation analysis was used to analyze strength of association between two variables. If data were non-parametric, they were rank-transformed and then analyzed using a one-way ANOVA. If a one-way ANOVA indicated a significant difference between all patient groups, Tukey's multiple comparisons test was used to determine differences between sets of two groups at a time.

Results

Initial Observations

Non-Disease Control vs. ALS

In control spinal cords, microglial populations were sparse with little to no microglial staining in some cases, specifically in the medial region of the left and right anterior horn (Figure 6b). The morphology was more-often rounded amoeboid (Figure 6d) microglia and microglia with small cell bodies and thin processes (Figure 6c). Microglia did not appear to cluster around motor neuron cell bodies (Figure 6e).

In ALS spinal cords, the microglial population was dense and evenly distributed throughout the anterior horn (Figure 7b). Microglial morphology ranged from small and rounded to large and fully ramified, and they appeared to have bulky cell bodies with thick processes (Figure 7c). The microglia clustered tightly around the remaining motor neurons, and some appeared to infiltrate the motor neuron cell bodies (Figure 7d).

The microglial population appeared to be both greater and more evenly distributed throughout the anterior horn in ALS compared to control spinal cords (Table 2). These data suggest that there are differences in the microglial population in ALS that are discernable even with non-quantitative evaluation of post-mortem spinal cords.

Quantitative Image Analysis

Initial results demonstrated observable differences in microglial populations in representative tissue sections from control and ALS spinal cords. Subsequent analysis was performed using the whole anterior horn of non-disease control, disease control and ALS patients to provide a more complete examination of the microglial population.

In order to investigate whether microglial populations show regional differences in microglial populations within the spinal cord we used the object count and positive pixel count methods to measure the abundance of microglia in cervical, thoracic, lumbar, and sacral sections from non-disease controls. A one-way ANOVA using object count for microglial population was used to analyze the effect of spinal region on the number of microglia (object count) in non-disease control. Results revealed a significant effect of spinal region on number of microglia ($F(3) = 6.846, p = 0.0004$) (Fig. 8a). To further investigate differences between specific regions of spinal cord, a post-hoc analysis via Tukey's multiple comparisons test was used. The results indicated a significant difference in object count between thoracic and lumbar regions ($p < 0.05$) and between thoracic and sacral regions ($p < 0.01$), with a greater number of microglia in the lumbar and sacral regions compared to the thoracic region. These results indicate that the number of microglia counted is contingent upon the region of spinal cord being analyzed.

We also addressed the issue of regional variability using the positive pixel count method. A one-way ANOVA using pixel score was used to assess the effect of spinal region on pixel score in non-disease control. Consistent with the results from object counts, there was an effect of spinal region on pixel score ($F(3) = 9.485, p < 0.0001$) (Fig. 8b). Post-hoc analysis via Tukey's multiple comparisons test confirmed significant differences in the positive pixel counts between thoracic and lumbar regions ($p < 0.0001$), with a greater pixel score in thoracic regions compared to lumbar regions. These results indicate that the proportion of spinal cord occupied by microglia is contingent upon the region of spinal cord being analyzed. Together, these data suggest that regional variation exists within the spinal cord of non-disease control patients. This data makes sense because the lumbar region of the spinal cord has a larger area than the thoracic region, and when obtaining object counts the area of the anterior horn was not taken into consideration. On

the other hand, when analyzing results from the positive pixel count, the total number of pixels (area) was utilized in the analysis. Since the region of interest is smaller in the thoracic cord, the proportion of the spinal cord taken up by microglia will be larger.

Microglial populations in ALS

The purpose of this analysis was to determine the variance of microglial populations in non-disease control and ALS patients using object count, positive pixel count, and object area. Due to the finding of regional differences present within non-disease control spinal cords, these analyses were conducted by comparing microglial populations by region, i.e. rostral (cervical and thoracic) and caudal (lumbar and sacral) regions of control and ALS spinal cord.

Rostral Spinal Cord (Cervical/Thoracic Regions)

Object Count

A one-way ANOVA analyzing the object count in non-disease control, disease control, and ALS patients in rostral spinal cord (cervical/thoracic) indicated that there was no significant difference in object counts between ALS and control patients ($F(3) = 1.945, p = 0.1590$) (Fig. 9a). These results indicate that there is no significant difference in the number of objects (microglia) in the rostral spinal cord of ALS patients, disease-control, and non-disease control patients.

Positive Pixel Count

A one-way ANOVA analyzing the positive pixel count in non-disease control, disease control, and ALS patients in rostral spinal cord (cervical/thoracic) indicated that there was no significant difference in pixel score between ALS and control patients ($F=1.813$, $p=0.1786$) (Fig. 9b). These results indicate that there is no significant difference in the pixel score (proportion of anterior horn of spinal cord occupied by microglia) in the rostral spinal cord of ALS patients, disease-control, and non-disease control patients.

Object Area

A one-way ANOVA analyzing the object area in non-disease control, disease control, and ALS patients in rostral spinal cord (cervical/thoracic) indicated that there was no significant difference in object counts between ALS and control patients ($F=2.99$, $p=0.0641$) (Fig. 9c). However, the data was trending towards significance and in a post-hoc analysis results revealed that the difference between non-disease control and ALS patients was trending towards significance ($p=0.0527$). To further assess the difference in microglial area between non-disease control and ALS patients, an unpaired t-test analyzing the object area in non-disease control and ALS patients in rostral spinal cord (cervical/thoracic) was applied. Results revealed a significant difference in object area between control and ALS patients ($t=2.195$, $p=0.0363$) (Fig. 10). These data suggest that the object area (microglial area) in the rostral spinal cord of ALS patients was significantly greater than in control patients.

Caudal Spinal Cord (Lumbar/Sacral Regions)

Object Count

A one-way ANOVA analyzing the object count in non-disease control, disease control, and ALS patients in caudal spinal cord (lumbar/sacral) indicated that there was a significant difference in object counts between the three groups ($F(3) = 3.243$, $p = 0.0257$) (Fig. 11a). The results of a post-hoc analysis revealed that the difference between non-disease control and ALS patients was trending towards significance ($p = 0.0576$). To further assess the difference in object count between non-disease control and ALS patients, an unpaired t-test analyzing the object count in non-disease control and ALS patients in caudal spinal cord (lumbar/sacral) was used. Results indicated that ALS patients had a significantly greater number of objects than control patients ($t = 2.777$, $p = 0.0250$) (Fig. 12a). These data suggest that ALS patients have significantly more microglial bodies occupying the caudal spinal cord compared to non-disease control spinal cord.

Positive Pixel Count

A one-way ANOVA analyzing the positive pixel count in non-disease control, disease control, and ALS patients in caudal spinal cord (lumbar/sacral) indicated that there was no significant difference in pixel score between the three groups ($F(3) = 4.863$, $p = 0.0879$) (Fig. 11b). The results of a post-hoc analysis revealed that the difference between non-disease control and ALS patients was trending towards significance ($p = 0.0670$). To further assess the difference in pixel score between non-disease control and ALS patients, an unpaired t-test analyzing the difference in pixel score in non-disease control and ALS patients in caudal spinal cord

(lumbar/sacral) was used. Results indicated that ALS patients had significantly greater pixel score than control patients ($t=2.123$, $p=0.0431$) (Fig. 12b). This data suggests that ALS patients have a significantly greater proportion of caudal spinal cord occupied by microglia.

Object Area

A one-way ANOVA analyzing the object area in non-disease control, disease control, and ALS patients in caudal spinal cord (lumbar/sacral) indicated that there was a significant difference in object area between the three groups ($F(3) = 7.113$, $p=0.0027$) (Fig. 11c). The results of a post-hoc analysis revealed that ALS patients have a greater object (microglial) area than non-disease control patients ($p=0.0043$). To further assess the difference in object area between non-disease control and ALS patients, an unpaired t-test analyzing the object area in non-disease control and ALS patients in caudal spinal cord (lumbar/sacral) was used. Results revealed a significant difference in object area between control and ALS patients ($t=4.228$, $p=0.0004$) (Fig. 12c). This data suggests that the object area in the caudal spinal cord of ALS patients was significantly greater than those in the control patients.

Stem Cell Positive vs. Stem Cell Negative Regions

Both injected (positive) and non-injected regions (negative) regions appeared to contain abundant microglial staining (Figure 13b); however, the positive region often contained focal regions seemingly cleared of microglia located in between dense clusters of microglia (Figure 13d). Microglia appeared to be both amoeboid and ramified with many thick processes in both the positive and negative regions; however, the relative abundance of microglia present was less in the region positive for stem cells. Clustering around motor neurons was apparent in both

regions, yet those motor neurons present in the centermost area of the positive regions were less likely to have clustering than those that were present in the lowermost area.

In several cases, the spinal cord region injected with stem cells exhibited noticeably less microglial staining than the region not injected; however, this was not true in all cases (Table 3). Both injected and non-injected regions appear to contain abundant microglial staining, but the injected region often contained sparsely stained regions located in between dense clusters of microglia. This data suggests there are heterogeneous microglial staining patterns in the patients that received the stem cell injection.

Initial results revealed heterogeneity in microglial staining patterns in patients that received the stem cell injection. Subsequent analysis was performed directed at the whole anterior horn of stem cell treated patients to provide a more complete examination of the microglial population. Stem cell injected tissue sections were divided into two groups: sections marked positive as showing the presence of stem cells in that section, and sections marked negative as presumably being absent of stem cells. Stem cell negative sections were chosen far from the spinal cord region that received the stem cell injection and having no observable stem cell clusters.

Stem Cell Positive vs Negative Object Count

A paired t-test analyzing the difference in object count in stem cell positive vs stem cell negative regions indicated that there was no significant difference in object count ($t=0.687$, $p=0.5094$) (Fig. 15a). This data suggests that there was no significant difference between stem cell positive and stem cell negative regions in the number of microglia in the anterior horn of the spinal cord.

Stem Cell Positive vs Negative Positive Pixel Count

A paired t-test analyzing the difference in positive pixel count in stem cell positive vs stem cell negative regions indicated that there was no significant difference in pixel score ($t=0.6115$, $p=0.5560$) (Fig. 15b). This data suggests that there was no significant difference between stem cell positive and stem cell negative regions in the proportion of the anterior horn of the spinal cord occupied by microglia.

Stem Cell Positive vs Negative Object Area

A paired t-test analyzing the difference in object area in stem cell positive vs stem cell negative regions indicated that there was no significant difference in object area ($t=0.4646$, $p=0.6532$) (Fig. 15c). This data suggests that there was no significant difference between stem cell positive and stem cell negative regions in the microglial area in the anterior horn of the spinal cord.

Time Elapsed from Stem Cell Injection to Death and Microglial Analysis

Object Count

A correlation analysis analyzing the strengths of association between time elapsed from date of stem cell injection to date of death and object count in stem cell positive regions indicated that there was a moderate, yet not statistically significant, association ($r=-0.552$, $p=0.1233$) (Fig. 16a). This moderate association indicated that when more time has elapsed from date of stem cell injection to date of death, the number of microglia in the spinal cord of stem cell positive regions decreases.

Positive Pixel Count

A correlation analysis analyzing the strengths of association between time elapsed from date of stem cell injection to date of death and pixel score in stem cell positive regions indicated that there was a strong and statistically significant association ($r=-0.8086$, $p=0.0083$) (Fig. 16b). This data suggests that when more time has elapsed from date of stem cell injection to date of death, the proportion of microglia occupying the spinal cord in stem cell positive regions decreases.

Object Area

A correlation analysis analyzing the strengths of association between time elapsed from date of stem cell injection to date of death and object area in stem cell positive regions indicated that there was a strong and statistically significant association ($r=-0.7596$, $p=0.0176$) (Figure 16c). This strong association indicated that when more time has elapsed from date of stem cell injection to date of death, the area of microglia in the stem cell positive regions of the spinal cord decreases.

Discussion

In order to examine how spinal cord and microglial populations differ in ALS as compared to controls, we analyzed microglial characteristics with a combination of quantitative measures. In addition, we investigated the microglial population in the spinal cords of ALS patients who received stem cell injections as participants in a clinical trial. The three quantitative measures used in this analysis, positive pixel count, object count, and object area, accounted for the proportion of microglial staining, the number of microglial cell bodies, and the morphology of microglia.

This is the first study to use quantitative methods to analyze microglial pathology in ALS. Previous studies have taken advantage of semi-quantitative categorical scoring and qualitative methods. In addition, to the best of our knowledge, this is the first study to examine the regional variability of microglia within non-disease control spinal cord.

Based on evidence from the positive pixel count, we can conclude that microglia in the caudal spinal cord in ALS patients cover a greater proportion of area in the anterior horn compared to non-disease controls. There was not enough evidence to conclude that rostral spinal cord in ALS patients exhibits this same increased proportion of microglia compared to non-disease control patients. These results suggest that ALS patients collectively exhibit higher levels of microglia (via pixel score) in the caudal spinal cord; however, this statement is contradicted by the data from cases 3, 6 and 13 (Table 4). These patients exhibited microglial pixel scores that were at or below the mean pixel score for non-disease control patients. Given that our results indicate that ALS patients have a higher *average* pixel score than non-disease control patients (ALS average = 11.50; Non-Disease Control average = 7.143), this suggests that microglia are only one factor that contributes to the inflammatory pathology of ALS.

Microglial number, as measured by object counts, showed that caudal spinal cord in ALS patients have a greater number of microglia compared to non-disease controls. In the rostral spinal cord, however, we did not observe the same increased number of microglia compared to non-disease control patients. Again, though ALS patients averaged a higher number of microglia in the caudal spinal cord (ALS average = 1248; Non-Disease Control average = 588.6), exceptions included cases 2, 5, 10, and 13 (Table 4), where microglial object counts were at or below the mean object count for non-disease controls. Our findings of an average increase in microglial presence in ALS are consistent with data from previous non-quantitative studies (Alexianu, 2001; Turner, 2004).

Microglia are only one of the cellular elements involved in neuroinflammation. Other potentially neuroinflammatory cells include astrocytes, macrophages, and infiltrating T-lymphocytes (Phillips, 2018). Astrocytes play a fundamental role in maintaining a low extracellular concentration of glutamate and secreting a variety of trophic factors, which have the ability to rescue motor neurons (Vargas, 2010; Dewil 2007). The dysfunction of astrocytes is suspected to drive ALS pathology through the loss of specific astrocytic glutamate transporters and a loss of neurotrophins. Additionally, reactive astrocytes can release toxic factors, which caused apoptosis of rat motor neurons (Pehar, 2004). Microglia, in coordination with other active glial cells and immune players, could explain why a greater number of microglia were not observed in all cases.

As compared to controls, we did not see a difference in microglial populations in the cervical and thoracic spinal cords of ALS patients. Of course, this may reflect too few cases to detect a difference, which might emerge with an increased sample size. Another possible explanation is that the cases included in our study may have had a higher burden of lower

extremity disease, which might be reflected in microglial activation in the lumbar cord. Indeed, previous studies have shown a relationship between microglial pathology and regional disease activity (Brettschneider, 2012). In a study of mSOD1 ALS mice, where the hindlimbs are preferentially affected, it was noted that protective and anti-inflammatory factors were increased in the cervical region compared with the lumbar region. Markers of inflammatory toxicity did not differ between cervical and lumbar regions in ALS mice, but T-lymphocytes infiltrated lumbar spinal cords before infiltrating the cervical region, suggesting that there may be an augmented protective response in the cervical spinal cord of ALS mice (Beers, 2011). The finding of regional variation in pathology has been noted in previous studies and further analysis of clinical variables and contributing factors is necessary to make a conclusion regarding the observed variation in the present study.

Microglial cells bodies were larger, as assessed by area measurement, in both the rostral and caudal regions of the spinal cord compared to non-disease control patients. The increase in the area of individual microglia likely reflects microglial activation. In their “resting” or “surveying” state, microglia, the resident innate immune cells in the brain, exhibit a morphology of a small-shaped soma and ramified processes characterized by extensive “fingers” that constantly monitor the surrounding environment by extending and withdrawing their processes (Davalos, 2005; del Rio Hortega, 1932; Nimmerjahn, 2005). The ramified morphology of microglia differs between varying regions of the brain (Lawson, 1990). Upon “activation”, microglia become de-ramified, a progression in which the number of processes and process length decline until reaching a state of amoeboid morphology (Kettenmann, 2011). In the activated state, microglia can be divided into classically activated microglia (M1) and alternatively activated microglia (M2). M1 microglia have been identified as those secreting

neurotoxic factors such as reactive oxygen species and pro-inflammatory factors, mediating motor neuron death (Zhao, 2004). In contrast, M2 microglia are thought to secrete anti-inflammatory cytokines and neurotrophins, enhancing motor neuron survival (Gordon, 2010). Microglia can become activated in response to any disturbance or loss of brain homeostasis such as infection, trauma, ischemia, neurodegenerative disease, or altered neuronal activity. Once in the amoeboid state, microglia become motile and can move to the location requiring attention (Kettenmann, 2011). The findings of the present study confirm the classic morphology of “activated” microglia and future identification of M1 vs M2 microglia would aid in further classifying the morphology associated with the continuum of microglia and their phenotypic characteristics.

Interestingly, we also found an increase in area in the caudal region of disease control patients compared to non-disease control patients. These disease controls were patients dying with Alzheimer’s disease. Inflammation also plays a role in the pathobiology of Alzheimer’s disease. The prominent pathological feature, amyloid- β , is able to bind and activate microglia and initiate the immune response, which can have differential effects on neuronal survival (Sastre, 2006a). While microglia may serve a beneficial, phagocytic role in the clearance of amyloid- β , they may also become over-activated and cause neuronal damage (Frauchy, 1998; Hickman, 2008). Previous literature indicates that increased microglial activation is observed in Alzheimer’s disease, and though spinal cord disease is not a feature of Alzheimer’s disease, a neuroinflammatory state may have contributed to the microglial pathology and morphology observed in this study’s non-disease control cases.

Analysis of the stem cell treated cases showed that there were no differences in microglial populations when comparing stem cell positive regions to stem cell negative regions.

There were trends, however, for a lower *average* positive pixel count and reduced average object area in stem cell positive regions indicating a potential difference in the proportion of anterior horn occupied by microglia, and the presence of smaller (less activated) microglia in patients treated with stem cells. Significant differences could possibly emerge with an increased sample size, which would suggest that the stem cell treatments were associated with fewer activated microglia, possibly indicating a therapeutic anti-inflammatory response to treatment.

An interesting finding was the presence of regions within the stem cell treated sections that that appeared to be cleared of microglia (Fig. 14). Certainly, these small areas of clearing might not be enough to significantly affect the pixel score or object count of the stem cell positive regions compared to the stem cell negative regions. However, they could reflect a local response to the presence of stem cells. Testing of this hypothesis will require formal “near neighbor” analysis of the relationship of microglia to the transplanted stem cells.

We performed a correlation analysis to investigate the strength of associations between time elapsed from date of stem cell injection to date of death with the three measures of microglial morphology in stem cell positive regions. In both the analysis of positive pixel count and object area, there was a strong and significant association of these measures with time since treatment. These results indicate that over longer periods of time, stem cell positive regions of spinal cord exhibited a lower proportion of microglia occupying the spinal cord and decreased microglia area. It is important to note that this analysis does not include time points from within a single patient’s lifetime, but is an analysis of an individual patient and their microglial population at their time of death. Furthermore, while a strong association was seen, all stem cell injected patients did die indicating that the injection of stem cells was not able to cure ALS, but the injection may have the ability to prolong life.

Limitations and Future Directions

The small sample sizes were one of the primary limitations of this study. This limitation was due largely to the number of patients within specific subject groups who were autopsied at Emory. While the ALS database at Emory is extensive, a major limitation was the time and resources available to complete this project.

Another potential limitation of this study was the accuracy of the computer software. While parameters within the software (both Aperio ImageScope and Image Pro Premier) were programmed to be as accurate as possible, the software still did make errors. For example, it occasionally did not detect a microglial cell body or would mislabel an artifact or blood vessel as a microglia. Furthermore, in some cases the background staining was much heavier and darker than in other cases and for this reason the software labeled more heavily.

A third limitation of this study was our inability to characterize the pro vs anti-inflammatory phenotypes of microglia. While we were able to analyze the area of microglia between subject groups, we were unable to determine morphological differences within a subject, which would aid in the study of the neuroprotective/neurotoxic distinction associated with M1 and M2 microglia. An interesting future direction would be the development of further morphological characteristics for a more complex analysis of microglial morphology within subjects.

This study laid the groundwork for future human studies focused on neuroinflammation and microglial pathobiology in ALS. In addition to repeating the present study with larger sample sizes, the inclusion of clinical data such as primary region of onset, and clinical characteristics at time of death would lend further insight into clinical factors that effect microglial activity. Furthermore, a future study in which antibodies that can identify factors

differentially secreted from M1 microglia, such as $\text{TNF}\alpha$, IL-6, IL-1 β , interferon- γ (IFN γ), and M2 microglia, such as IL-4, IL-10, YM1, and CD206, could lend further insight into the cytotoxic pathological progression as ALS advances. Such a study would make it possible to determine the cytotoxic elements contributing to a degenerative aspect of ALS, which would make possible the development of a therapeutic treatment for the suppression of these cytotoxic factors.

Another interesting direction to pursue is to create further methods to characterize the morphology of microglia via object roundness and numbers of microglial processes to better assess the “type” of microglia present within stem cell positive and negative regions. Using methods in which antibodies can identify neurotoxic or neuroprotective factors secreted from microglia would further aid in the identification of the microglia present in the anterior horn of the spinal cord and surrounding motor neurons. This future study would make it possible to better understand the effects that an injection of neural stem cells has on the immune environment in ALS.

The present study provides a foundation for future research to further examine microglial populations in human ALS. Microglia is a hallmark of neuroinflammation and the suppression of its neurotoxic effects and reinforcement of its neuroprotective effects make it a promising pharmacological target for the treatment of ALS. Better understanding of the relationship between pathology and morphology of microglia will aid in the development of directed treatment options for both ALS and other diseases that exhibit neuroinflammation.

Figures and Tables

Characteristic	Total (n=38)	Non-Disease Control (n=7)	Disease Control (n=7)	ALS (n=14)	ALS/Stem (n=10)	Statistical Value	P Value
Gender (Male: Female)		4:3	4:4	7:7	7:2	-	-
Post Mortem Interval		9.4±6.1	22±16.0	13.86±6.7	10.6±4.9	3.157	0.0372
Age at onset, mean (SD), years		-	58.5±19.9	56.4±7.7	54.2±5.3	0.2951	0.7469
Age at death, mean (SD), years		84.9±9.0	67.4±16.2	59.6±7.2	57.7±5.4	14.21	<0.0001
Disease duration, mean (SD), years		-	10.33±3.5	3.4±2.4	1.6±1.2	27.89	<0.0001

Table 1. Disease characteristics for the four subject groups. The statistical test used to evaluate differences in the means between subject groups was a one-way non-parametric ANOVA. Significance was evaluated at the $P < 0.05$ level. Statistical significance was found in post mortem interval, age at death, and disease duration. Tukey's multiple comparisons test was used to determine differences between sets of two groups. The difference in post mortem interval of non-disease control and disease control was significant ($p=0.0467$). The difference in age of death between non-disease control and the three other disease subject groups was significant ($p=0.0072$; $p<0.0001$, $p<0.0001$). The difference in disease duration between disease control and ALS and ALS/Stem was significant ($p<0.0001$, $p<0.0001$).

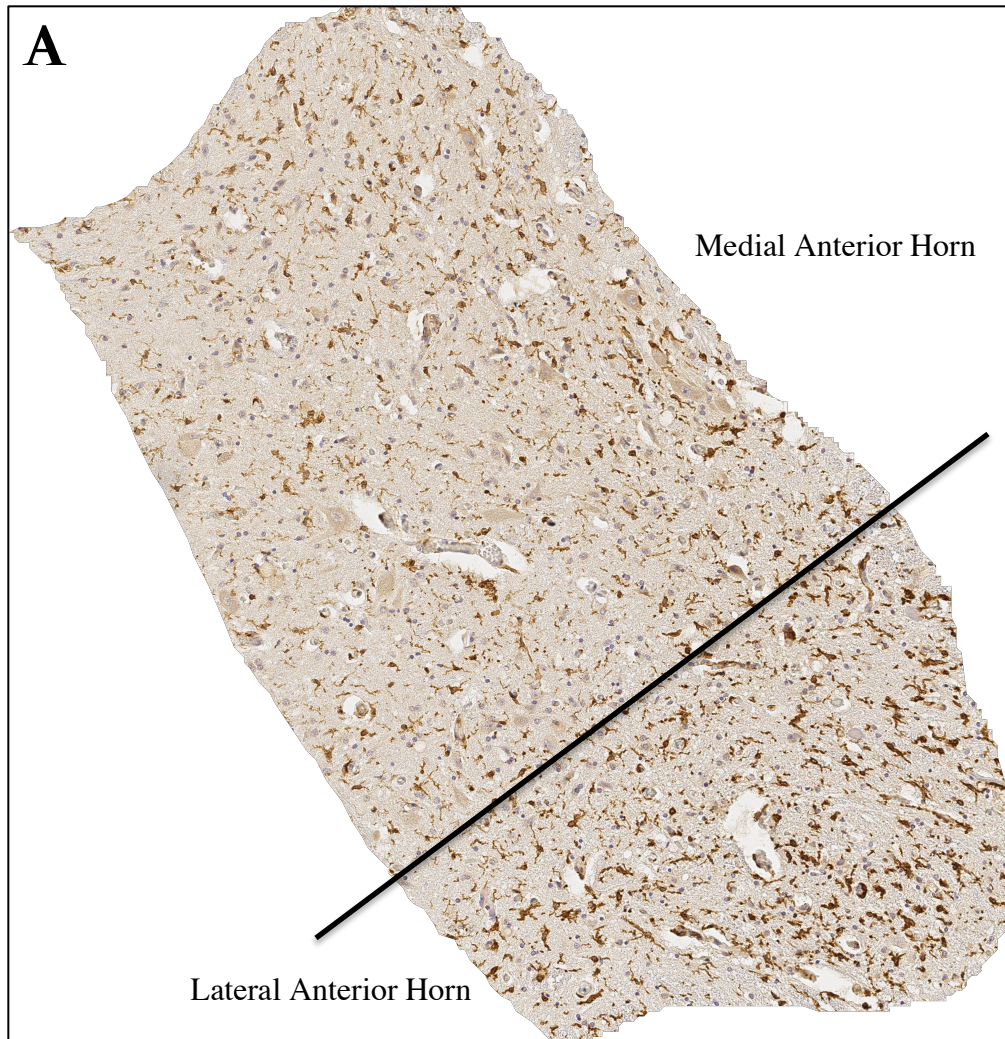


Figure 1. Differences in density of microglial populations noted between medial and lateral anterior horn. An example of the differences noted within the anterior horn in the initial analysis of the microglial populations.

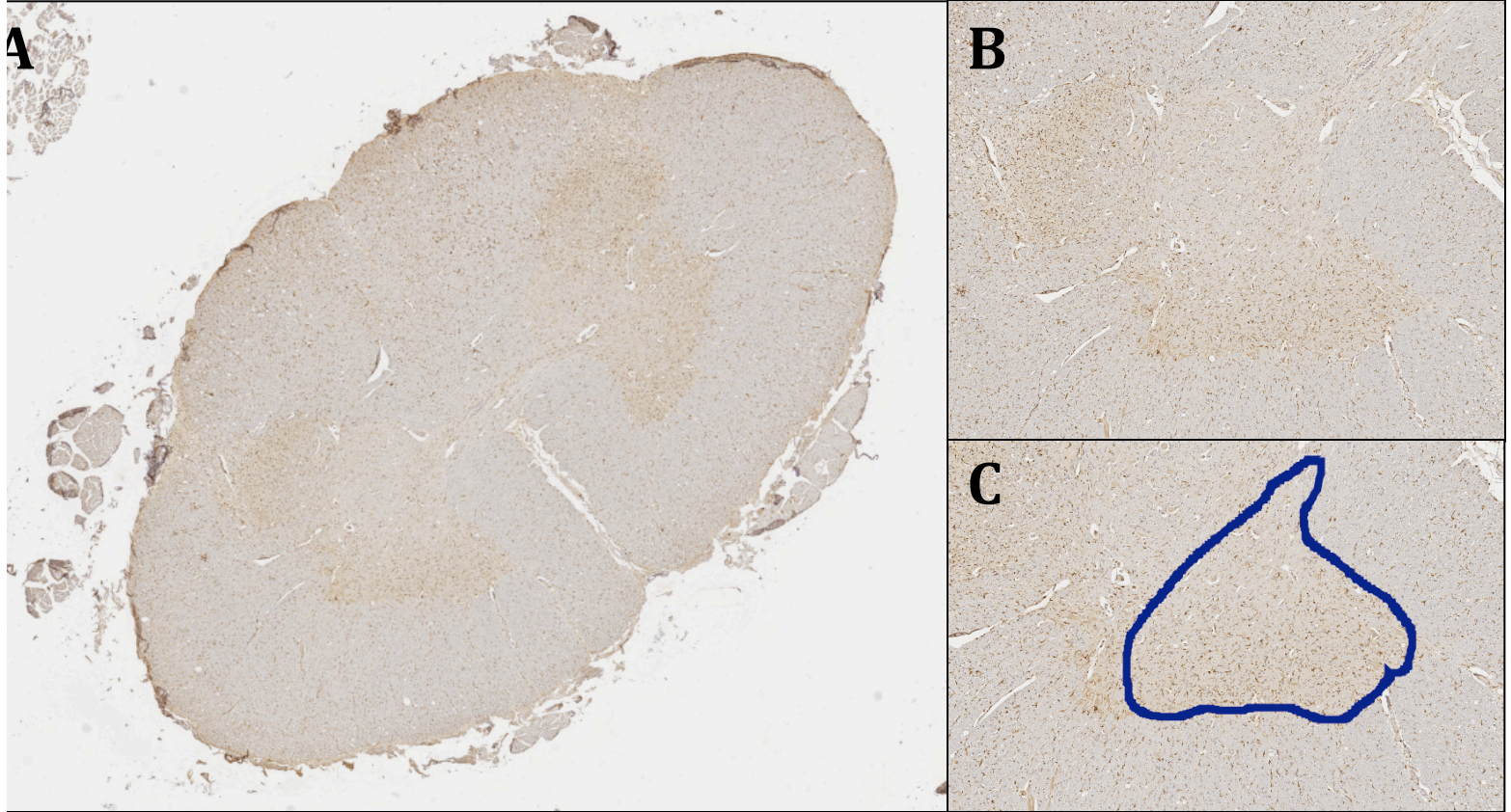


Figure 2. Annotating the region of interest (anterior horn) in Aperio ImageScope. A. A thoracic section of spinal cord from case (XX). **B.** The left anterior horn (target region) surrounded by white matter (non-target region). **C.** The free-form annotation encompassing the left anterior horn (target region), which will subsequently be used for analysis.

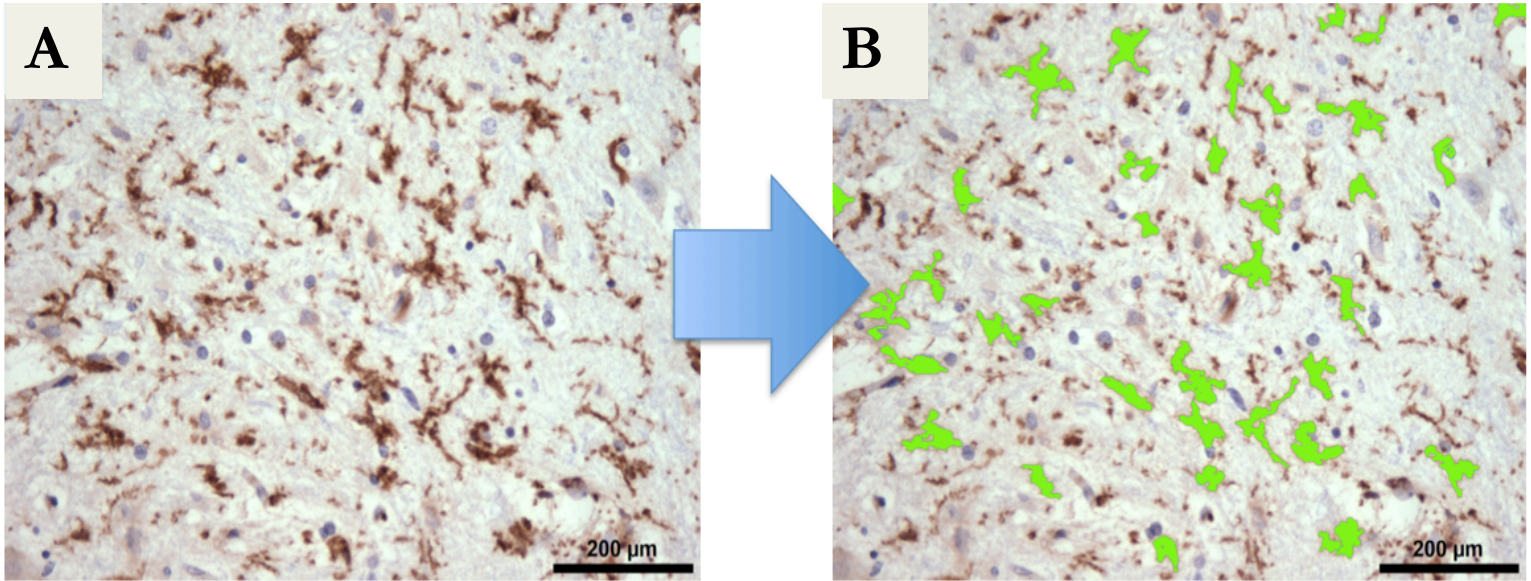


Figure 3. Quantitative analysis of microglia using the object counts. An example of the pre and post-analysis images used for the counting procedure for quantitative analysis of microglia numbers. (a) The pre-analysis image shows the microglial abundance in the lateral region of the right anterior horn. (b) The post-analysis image shows the microglial masks that were used to create the object counts.

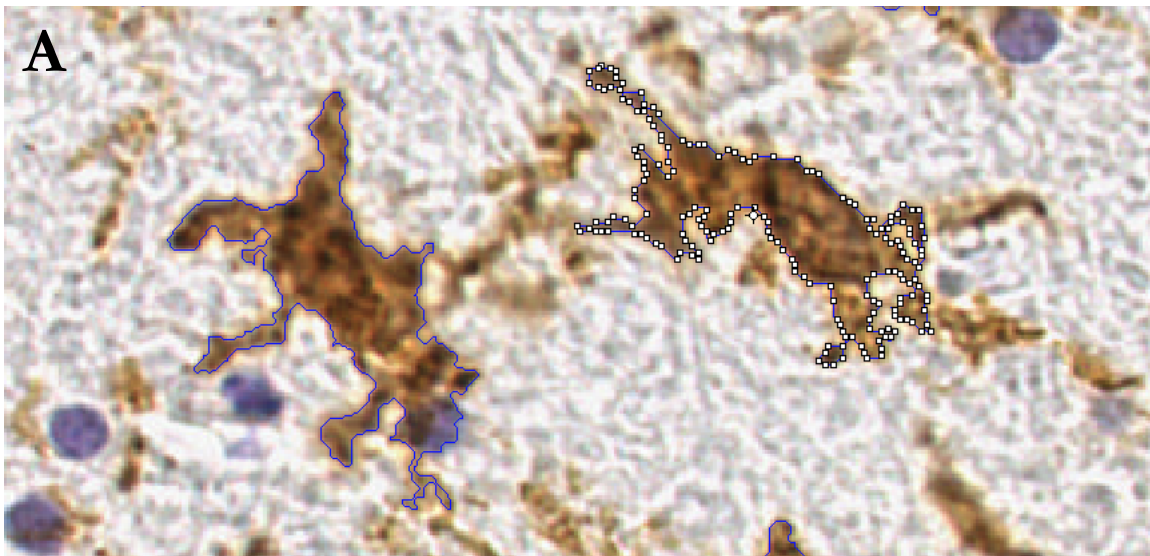


Figure 4. Quantitative analysis of microglia using the object area. An example of the outlines created via the object masks to calculate the area of microglia. A. A microglial cell body and its processes outlined via parameters of the software for the analysis of microglial area.

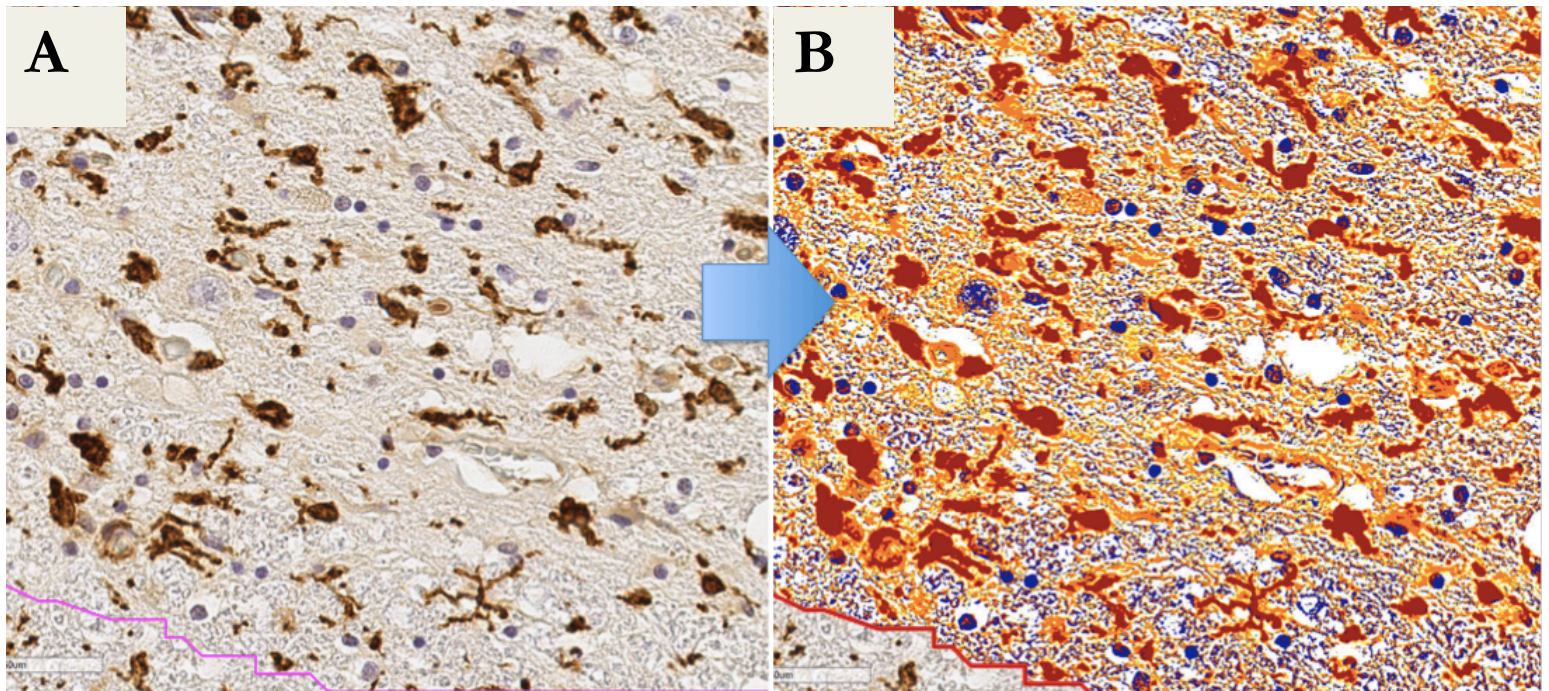


Figure 5. Quantitative analysis of microglia using positive pixel count. An example of pre and post-analysis images of the positive pixel count algorithm used for quantitative analysis. **(a)** The pre-analysis image shows the microglial abundance (brown) before software analysis was applied. **(b)** The post-analysis image exhibits the color quantification of each pixel. Blue: negative; Yellow: weak-positive; Orange: positive, Red: Strong-positive.

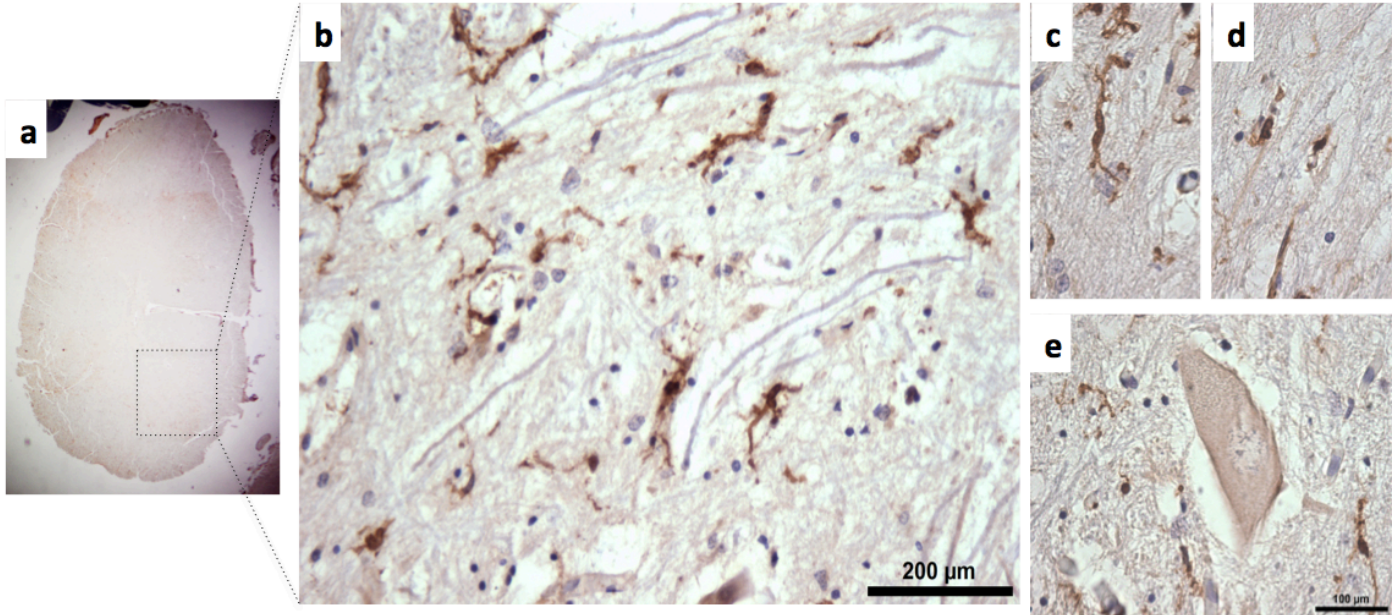


Figure 6. Qualitative analysis of microglial populations in control spinal cords. Non-disease control spinal cords exhibit fewer microglia in the anterior horn than ALS spinal cord. **(a)** The lumbar section of control spinal cord of case 5 (1X). **(b)** The left lateral region of the anterior horn displays the relative sparseness of microglia distributed in this section (20X). **(c)** Microglia with small cell bodies and long, thin processes and **(d)** rounded amoeboid microglia represent the most common morphology present in control spinal cord (40X). **(e)** Microglial clustering is not apparent around motor neurons present in the medial anterior horn (40X).

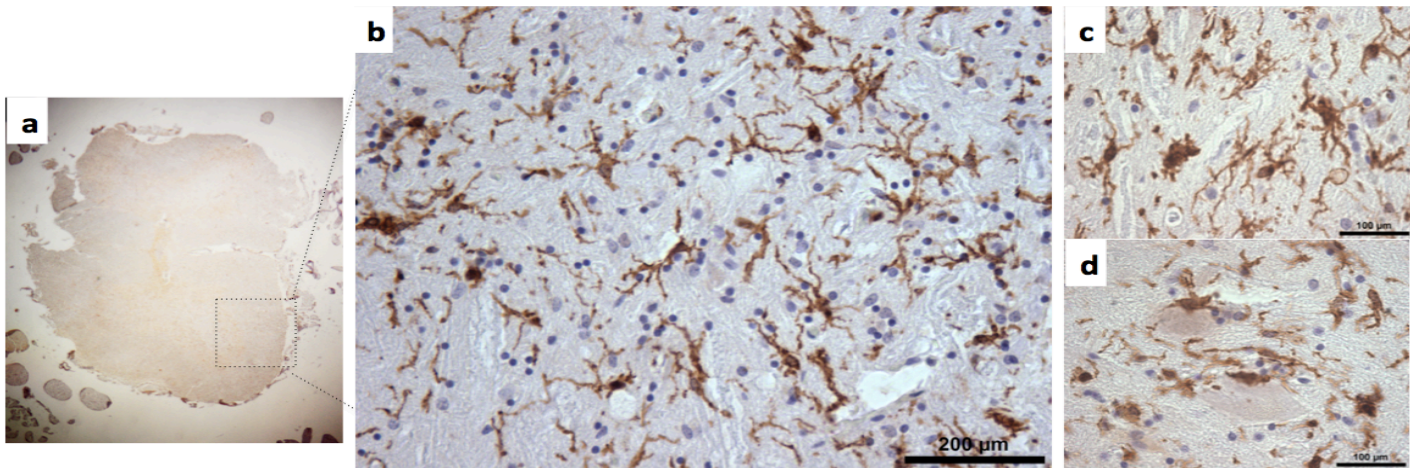


Figure 7. Qualitative analysis of microglial populations in ALS spinal cords. ALS spinal cords exhibit increased numbers of microglia in the anterior horn with different morphologies than control spinal cord. **(a)** The lumbar section of ALS spinal cord of case 4 (1X). **(b)** The left lateral region of the cord displays the relative abundance of microglia distributed in this section (20X). **(c)** Fully ramified microglia with large cell bodies and thick processes are identified as the major morphological specimen in ALS spinal cord (40X). **(d)** Microglia are heavily clustered around motor neurons in the medial anterior horn (40X).

Control					
Region	Case #	LeLa	LeMe	RiLa	RiMe
Thoracic	1	+	+	+	+
Lumbar		+	+	+	+
Thoracic	2	++	++	++	++
Lumbar		+	+	++	+
Thoracic	3	+	+	++	+
Lumbar		+	+	+	+
Sacral		++	+	+	+
Thoracic	4	+	+	+	+
Lumbar		+	+	+	+
Sacral		+	+	+	+
Thoracic	5	++	++	++	++
Lumbar		++	++	++++	+
Sacral		++	++	++	+

ALS					
Region	Case #	LeLa	LeMe	RiLa	RiMe
Cervical	6	+	+	++	+
Thoracic		++	++	+	+
Cervical	7	+++	++++	n/a	n/a
Thoracic		++++	++++	+++	+++
Lumbar		+++	++++	++++	+++
Sacral		++++	++++	++++	+++
Thoracic	8	+	+	+	++
Lumbar		++++	+++	n/a	n/a
Sacral		++	+	+++	++
Cervical	9	+	+	+	+
Thoracic		++	+	+++	+
Lumbar		+	+	+	+
Thoracic	10	++++	++++	++++	++++
Lumbar		++++	+++	++++	++
Sacral		++++	++	++	+

Table 2. A summary table of an initial analysis of non-disease control vs ALS spinal cords. Quantitative results from the microglial population in the anterior horn of lumbar, thoracic, sacral, and cervical spinal cord regions were categorized as ≤ 20 (+), 21-31 (++), 32-42 (+++), and ≥ 43 (++++). LeLa: left lateral; RiLa: right lateral; LeMe: left medial; RiMe: right medial. The regions in the table represent available sections. Boxes in grey represent unavailable sections. Results are displayed as a heat map. **(a)** Control summary table displaying the results of 5 control cases. **(b)** ALS summary table displaying the results of 5 ALS cases.

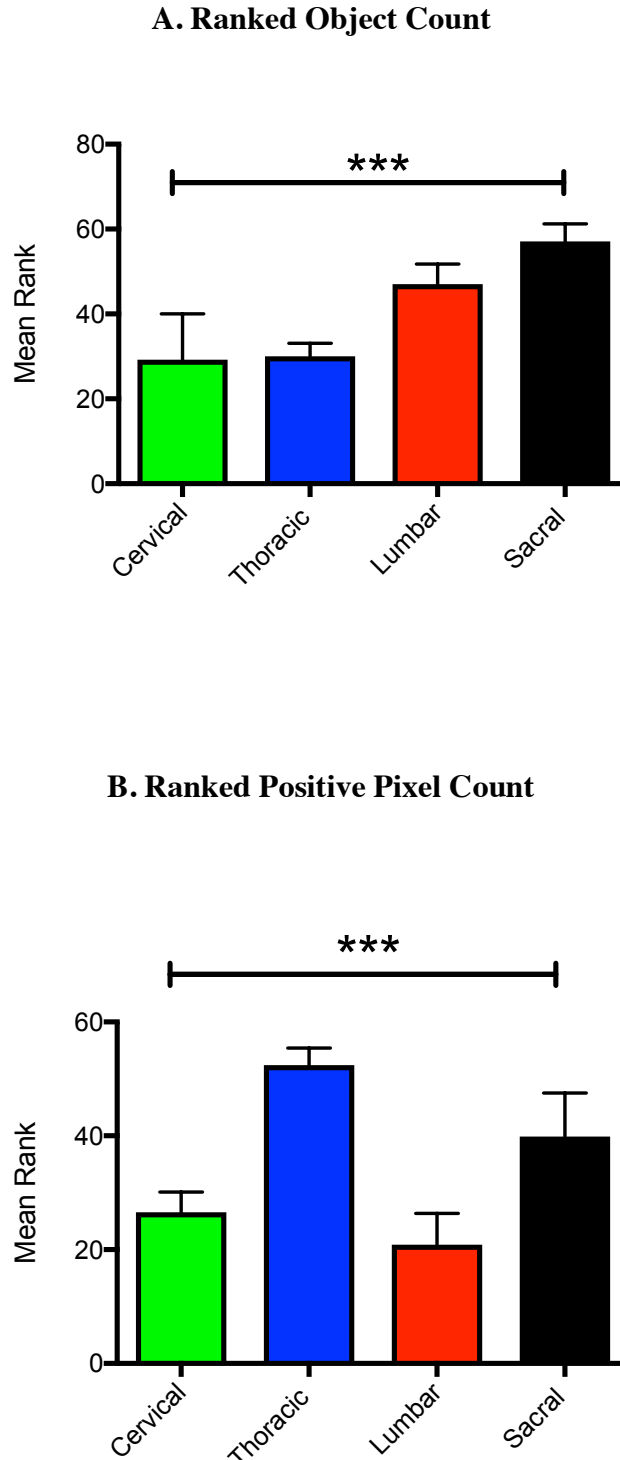


Figure 8. Microglial population analyses within varying regions in non-disease control spinal cord. A. Region of spinal cord was found to have a significant effect on the number of microglia present within the anterior horn. Post-hoc analysis indicated a significant difference between thoracic and lumbar regions and between thoracic and sacral regions. Bars represent mean object number \pm SEM. **B.** Region of spinal cord was found to have a significant effect on the positive pixel count within the anterior horn. Post-hoc analysis indicated a significant difference between thoracic and lumbar regions. Bars represent mean pixel score \pm SEM.

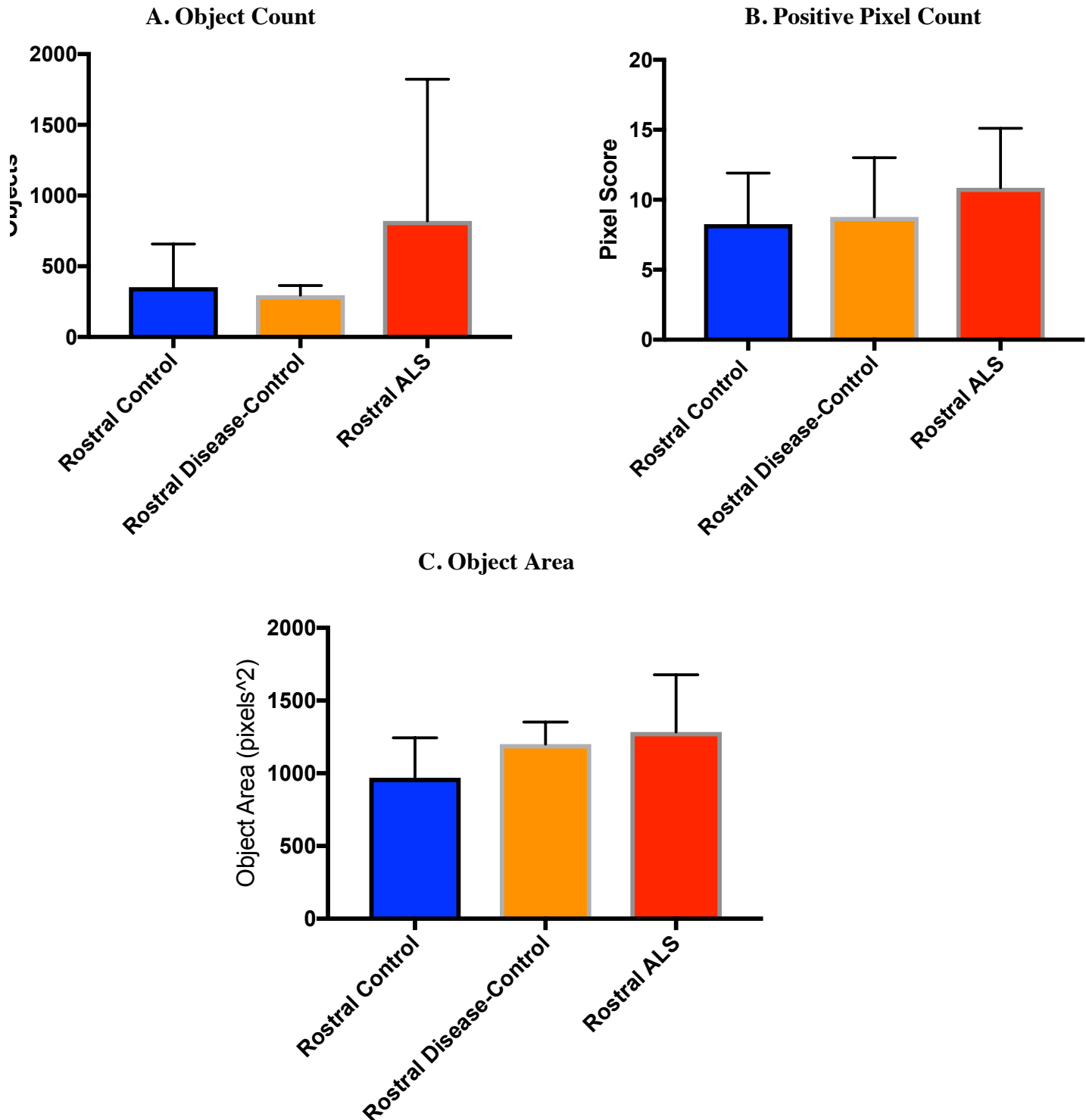


Figure 9. Microglial analyses of the rostral spinal cord in non-disease control, disease control and ALS patients. **A.** There is no significant difference in the number of microglia present between non-disease control, disease control, and ALS patients. Bars represent mean object number \pm SEM. **B.** There is no significant difference in the pixel score between non-disease control, disease control, and ALS patients. Bars represent mean pixel score \pm SEM. **C.** There is no significant difference in the microglial area between non-disease control, disease control, and ALS patients; however, the difference between microglial area in non-disease control and ALS patients is trending towards significance ($F=2.744$, $p=0.0634$). Bars represent mean object area \pm SEM.

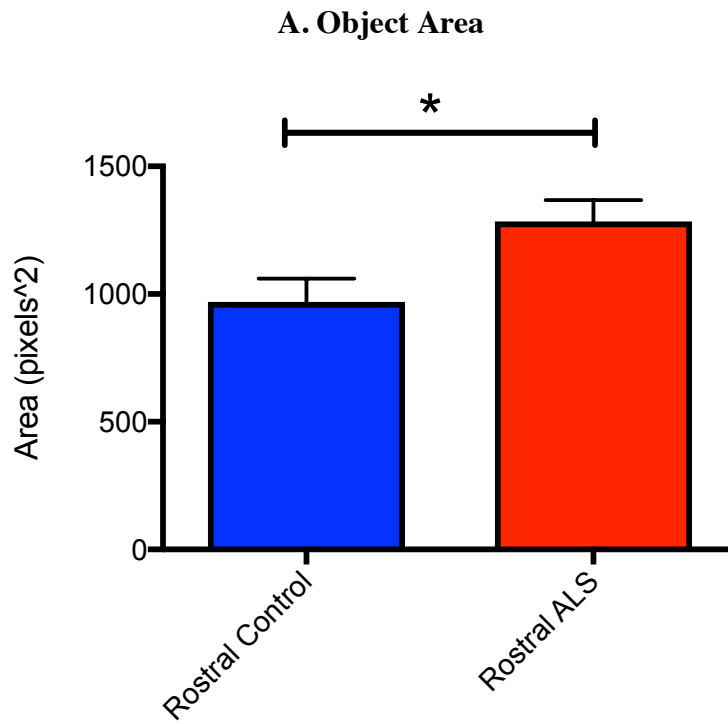


Figure 10. Analysis of microglia area in the rostral spinal cord in non-disease control and ALS patients. A. ALS patients exhibit a significantly greater microglia area when compared to non-disease control patients. Bars represent mean object area \pm SEM.

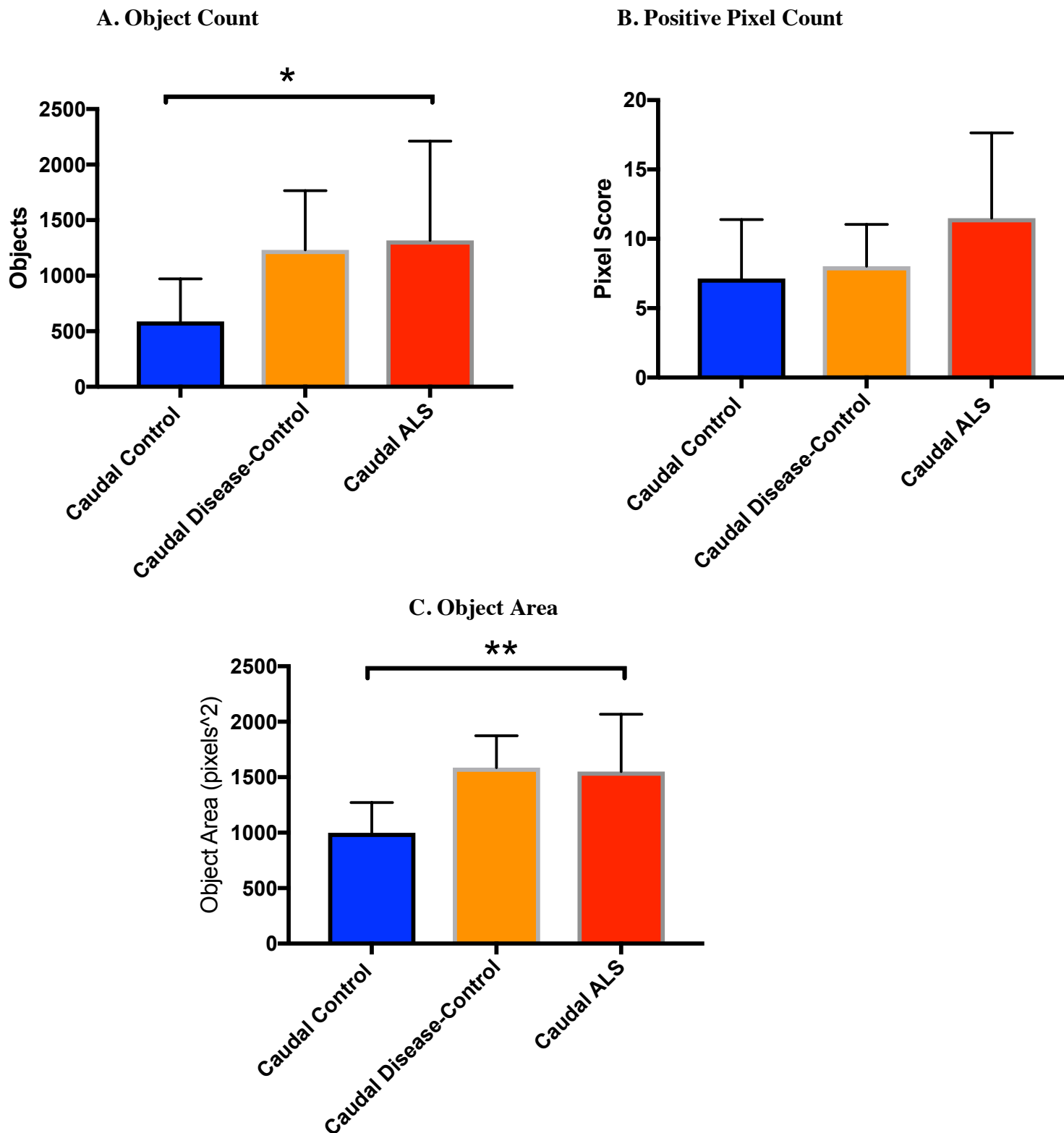


Figure 11. Microglial population analyses of the caudal spinal cord in non-disease control, disease control and ALS patients. **A.** There is no significant difference in the number of microglia present between non-disease control, disease control, and ALS patients. Bars represent mean object **A**. **ALS patients exhibit a significantly greater microglia area when compared to non-disease control patients.** Bars represent mean object area \pm SEM. **B.** There is no significant difference in the pixel score between non-disease control, disease control, and ALS patients. Bars represent mean pixel score \pm SEM. **C.** The microglial area in ALS patients is significantly greater than in non-disease control patients. Bars represent mean object area \pm SEM.

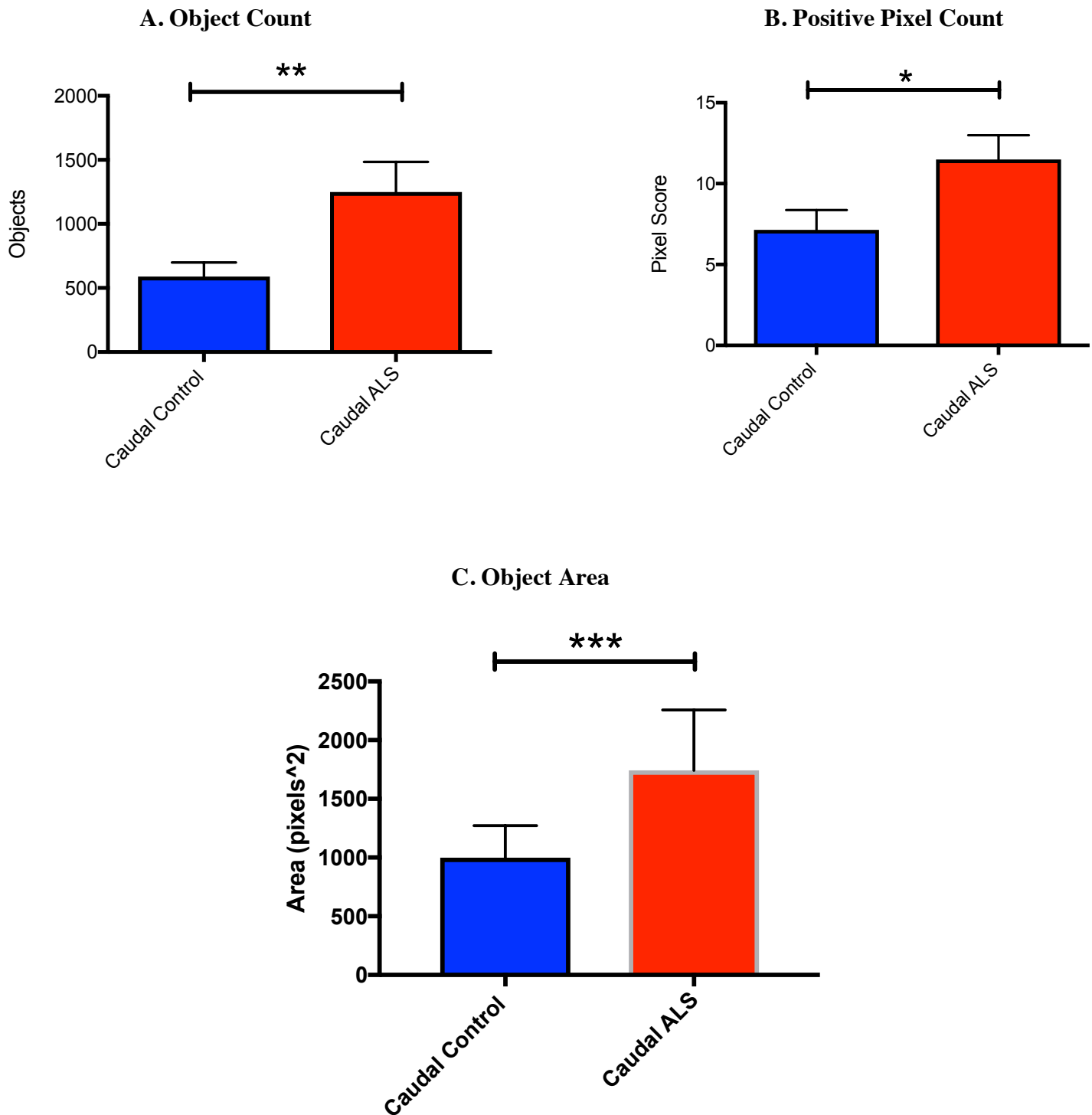


Figure 12. Microglial population analyses of the caudal spinal cord in non-disease control and ALS patients. **A.** ALS patients exhibit a significantly greater proportion of spinal cord occupied by microglia when compared to non-disease control patients. Bars represent mean object number \pm SEM. **B.** ALS patients exhibit a significantly greater number of microglia present in the anterior horn of the caudal spinal cord when compared to non-disease control patients. Bars represent mean pixel score \pm SEM. **C.** ALS patients exhibit a significantly greater microglia area when compared to non-disease control patients. Bars represent mean object area \pm SEM.

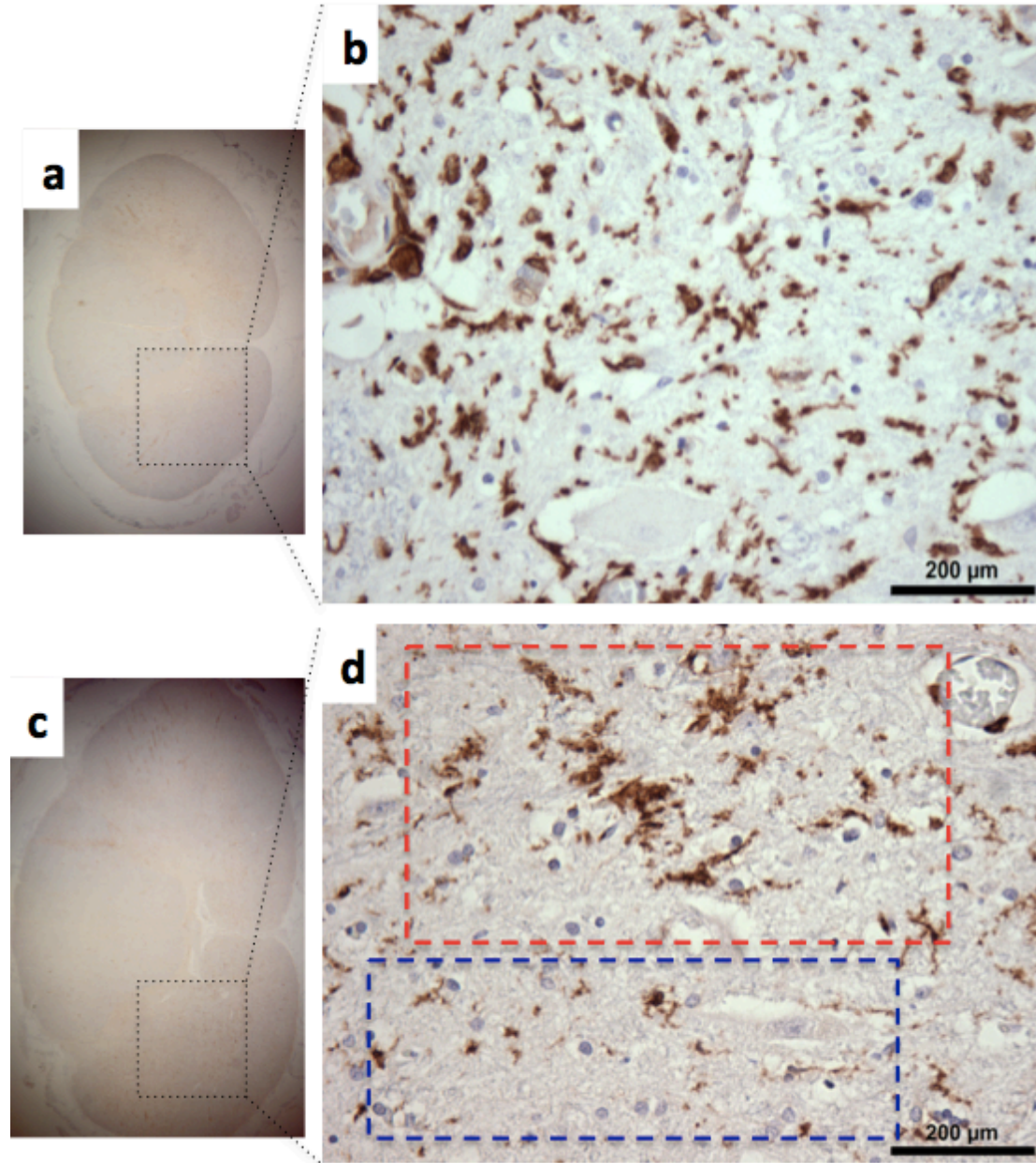


Figure 13. A comparison of injected and non-injected spinal cord regions in case 5. (a) Thoracic section; a region not injected with stem cells (1X). **(b)** The left lateral region of the anterior horn displays a great abundance of microglia very evenly distributed throughout the anterior horn (20X). **(c)** Cervical section; injected with stem cells (1X). **(d)** The left lateral region of the anterior horn displays an abundance of microglia, and also the clear clustering of microglia in this section (20X). The region boxed in red displays one of these clusters of microglia, and the region boxed in blue exhibits an area of relatively sparse microglia.

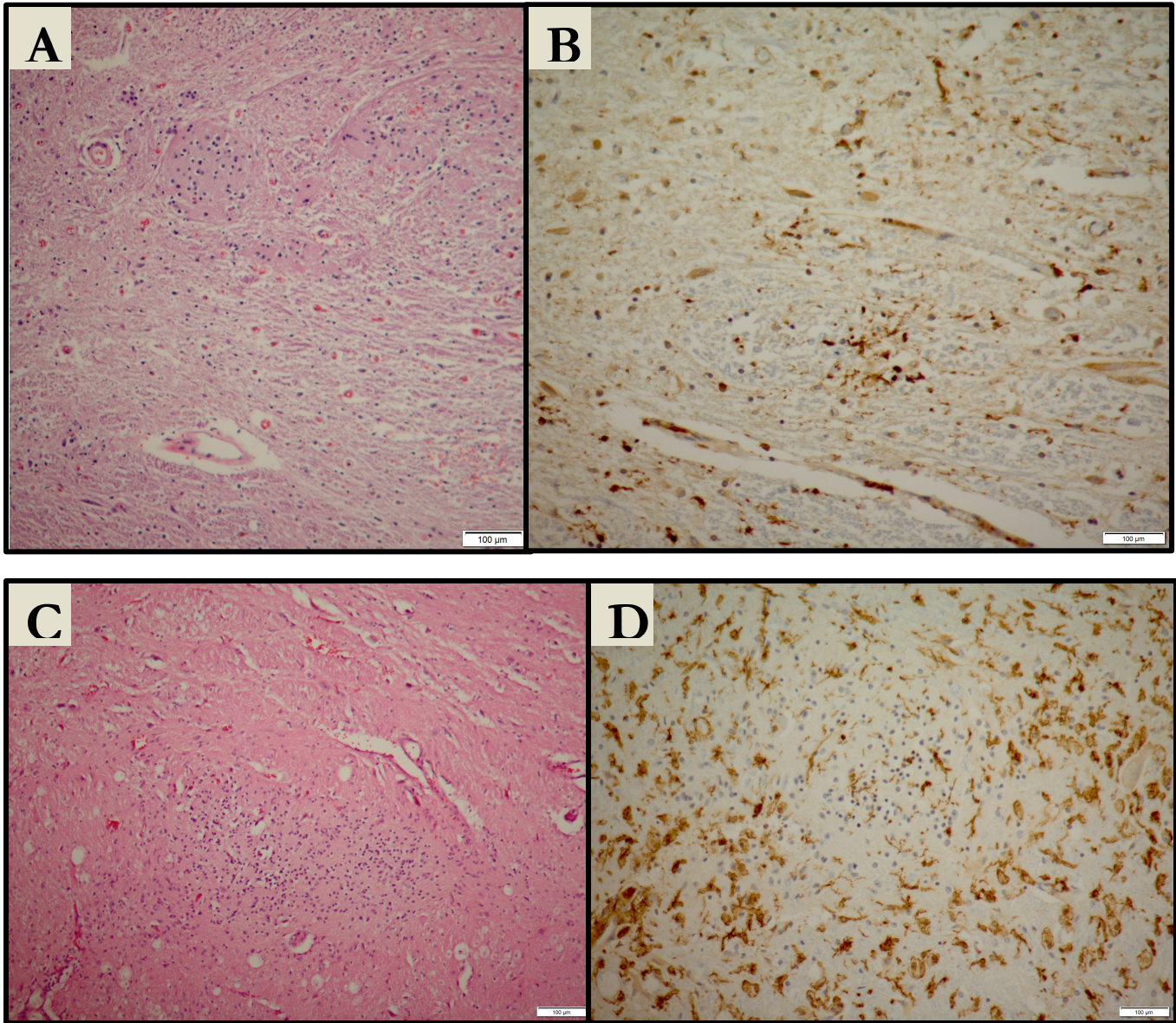


Figure 14. Stem cell treated sections of spinal cord exhibit regions of clearing. A. Haematoxylin and Eosin (H&E stain used for the visualization of cell nuclei shows a cluster of cell nuclei, possibly stem cells in case 6. **B.** Iba1 stain used for the visualization of microglia shows the corresponding section cleared of microglia in case 6. **C.** H&E stain used for the visualization of cell nuclei shows a cluster of cell nuclei, possibly stem cells in case 8. **D.** Iba1 stain used for the visualization of microglia shows the corresponding section cleared of microglia in case 8.

Region	Case #	Stem Cell Negative				Stem Cell Positive			
		LeLa	LeMe	RiLa	RiMe	LeLa	LeMe	RiLa	RiMe
Lumbar	11	++	+	+	++	++	++	+++	+
	12	++	+	++	+++	+	+	+	+
	13	+	++	++	++	+++	+	++	+
	14	+	+	+	+	++	+	+++	+
Cervical	15	+	+	+	+	+	+	+	+
	16	++++	+++	+++	++	+++	++	+++	+
	17	++	++	+	+	++	+	++	+
	18	++++	++++	++++	++++	+++	++	++++	+++
	19	+++	++	+++	+	+	+	++	+

Table 3. A summary table of an initial analysis of stem cell positive vs negative regions. Quantitative results from the microglial population in the anterior horn of each spinal cord region were categorized into ≤ 20 (+), 21-31 (++), 32-42 (+++), and ≥ 43 (++++). Cases 11-14 display results for patients who received a lumbar injection of stem cells, and cases 15-19 display the results for patients who received a cervical injection. LeLa: left lateral; RiLa: right lateral; LeMe: left medial; RiMe: right medial. Results are displayed as a heat map.

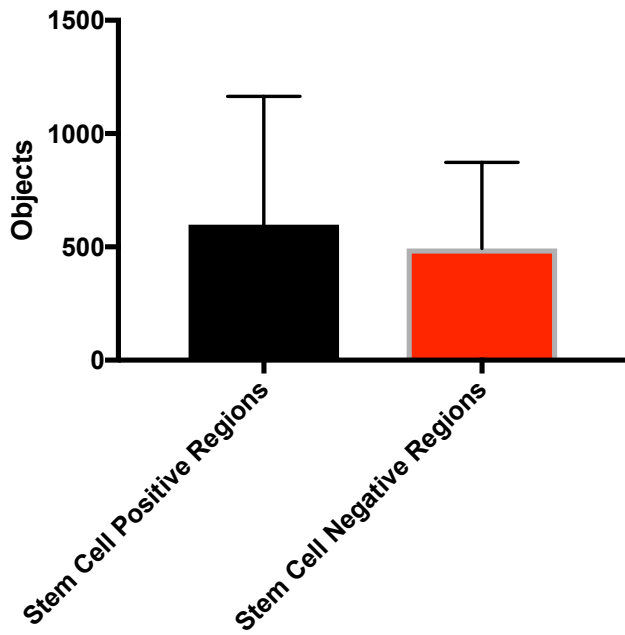
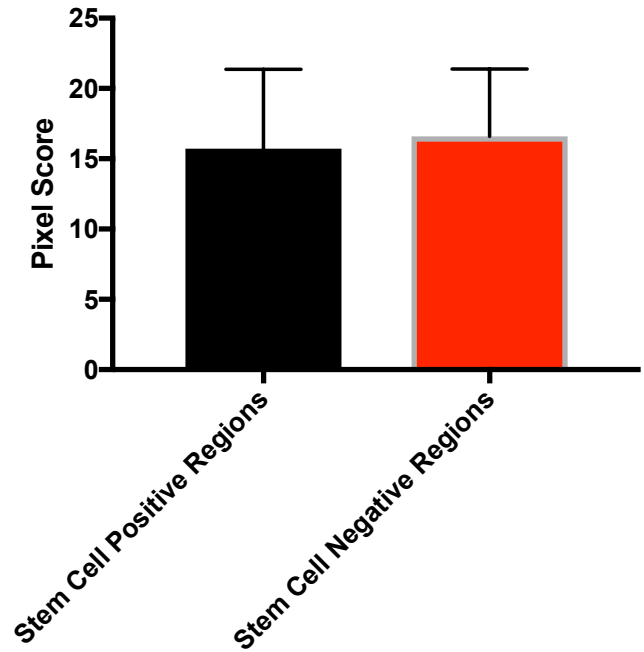
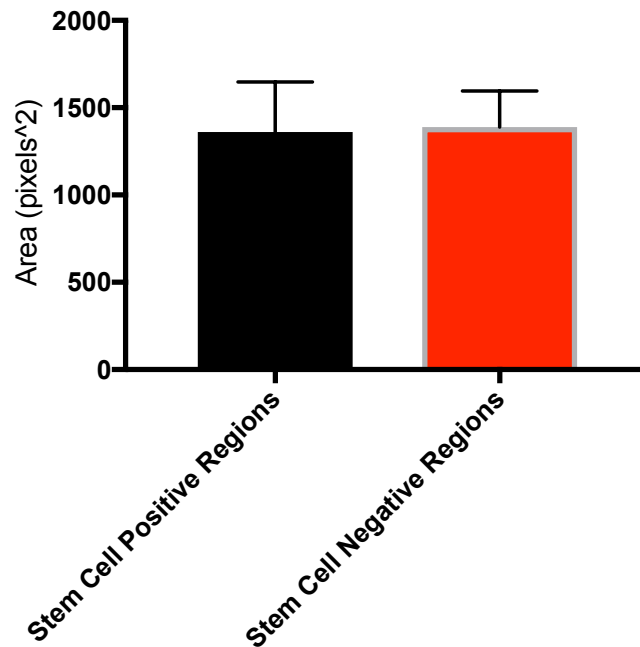
A. Object Count**B. Positive Pixel Count****C. Object Area**

Figure 15. Microglial population analyses of stem cell positive vs negative regions. **A.** There is no significant difference in the number of microglia present in stem cell positive vs negative regions. Bars represent mean object number \pm SEM. **B.** There is no significant difference in the positive pixel count in stem cell positive vs negative regions. Bars represent mean pixel score \pm SEM. **C.** There is no significant difference in the area of microglia in stem cell positive vs negative regions. Bars represent mean object area \pm SEM.

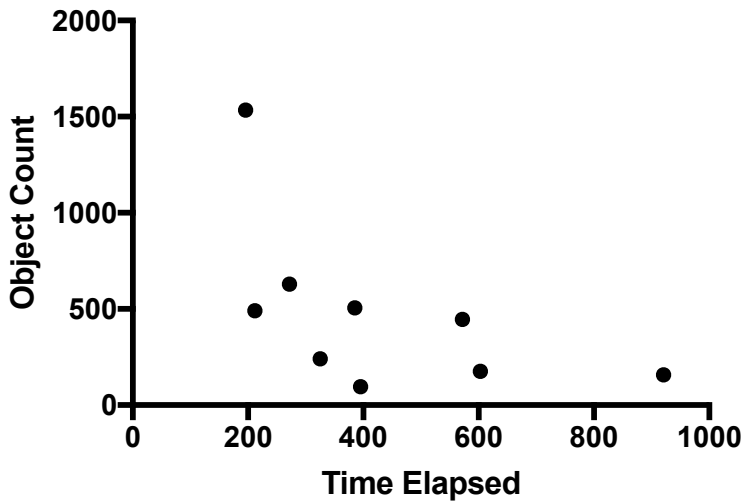
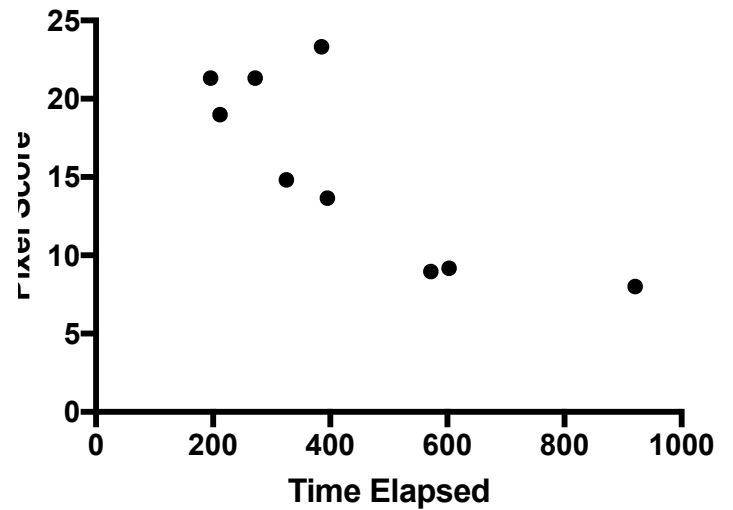
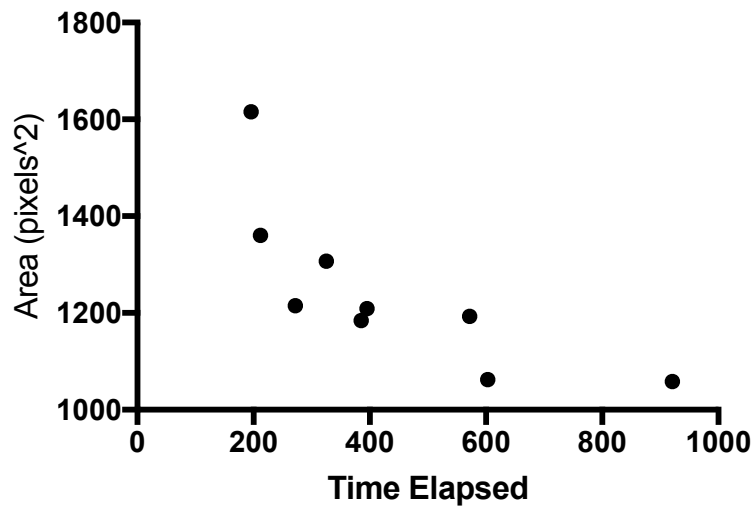
A. Object Count**B. Positive Pixel Count****C. Object Area**

Figure 16. Correlation analyses within stem cell positive regions. Time elapsed from date of stem cell injection to date of death and microglial measures were analyzed. **A.** A moderate negative correlation between time elapsed and number of microglia present in stem cell positive regions. **B.** A strong negative correlation between time elapsed and proportion of spinal cord occupied by microglia. **C.** A strong negative correlation between time elapsed and area of microglia.

Case Number	Rostral Pixel Score	Caudal Pixel Score	Rostral Object Count	Caudal Object Count	Rostral Object Area (pixels ²)	Caudal Object Area (pixels ²)
1	6.61	3.00	36.00	52.50	311.67	437.47
2	12.58	9.54	537.75	1062.00	838.21	922.57
3	9.25	7.64	272.30	376.67	960.13	778.905
	12.90	2.35		211.5		1035.94
4	12.63	11.16	566.22	1018.75	1056.75	1416.36
		8.78		1082		1056.75
5	9.41	7.16	998.00	816.33	1040.47	1056.445
		12.21		1017		1132.12
6	3.84	2.10	89.9	281.6	990.072	974.026
	4.99	3.46	141	304	1173.405	756.1833
7	7.05	3.66	194.36	322.5	1262.94	1141.11
	3.87	14.64	334	518.5	1086.33	1316.46
1	4.34	4.21	209.86	553.17	1203.47	1251.55
2	8.47	8.33	313.90	1311.50	1224.20	1359.01
3	5.60	3.69	286.00		940.73	1323.50
4	8.78	11.34	364.83	1704.40	1161.29	1489.62
5	7.71	5.87	256.33	942.33	1420.01	7.72
6	9.03	6.58	400.38	712.25	1396.15	1598.70
7	17.51	10.91	244.88	2038.25	1281.70	2101.07
		10.62		1359.5		1802.61
1	10.63	7.27	460.17	1586.25	1078.88	1354.61
		8.39		465.33		695.56
2	14.81	10.72	546.67	574.5	1175.38	1060.71
				2109.5		1600.61
3	7.12		269		792.66	
	16.55		173.67		1384.815	
4	14.37	11.78	2155	2174.5	868.475	1340.28
	10.25	17.08	769.5	2327	1088.458	1171.73
5	7.49		244.5		954.21	
	12.07	11.87	207.5	502.00	947.16	1171.72
6	4.94	9.06	189.92	1177.50	1414.07	1191.278
		2.11				1404.49
7	16.55	20.83	507.5	3188.75		2366.448
	14.64	22.98	744.5	1460.52	1719.73	2459.83
8	9.16		4190		1742.52	
	10.89		1374		1211.303	
9	15.32		2498.50		2047.26	
10	17.74	11.25	1032.00	2069.00	2082.04	2444.847
						1945.54
11	10.98	17.60	428.50	569.5	1460.00	1729.24
		16.21				1573.415
12	11.56		473.14	1748.50	1601.792	1792.61
	7.58	9.42			1494.835	
13	7.91		237.83		1134.14	
14	3.57	2.43	145.25	481	812.6811	1199.50
	3.77	2.64	316.5	165	902.98	

Table 4. Quantitative analysis results for individual non-disease control, disease- control and ALS cases. Control cases without disease are represented in blue, control cases with disease are represented in orange, and ALS cases are represented in red. Quantitative analysis results from rostral and caudal regions of the spinal cord for positive pixel count, object count, and object area are listed. When no number is listed, the corresponding section was either not available or damaged in the immunohistochemistry staining process.

Assigned Number	Positive Pixel Score	Negative Pixel Score	Positive Object Count	Negative Object Count	Positive Object Area (pixels ²)	Negative Object Area (pixels ²)	Time Elapsed from Injection to Death (days)
1	21.33	23.08	629.00	328.17	1214.97	1432.29	272
2	13.66	14.54	95.50	16.25	1760.46	1420.01	395
3	14.83	20.69	240.00	477.25	1306.95	1279.62	325
4	8.97	10.24	446.50	243.50	1192.87	1252.39	572
5	8.01	11.70	158.33	279.00	1058.06	1098.07	921
6	21.31	21.74	1534.50	422.00	1615.94	1467.78	196
7	9.18	14.31	176.33	953.50	1062.58	1258.63	603
8	18.99	11.39	490.17	352.67	1360.03	1329.34	212
9	23.32	17.10	505.25	522.67	1184.30	1476.89	385
10	17.59	21.08	1700.00	1332.50	1858.94	1872.24	

Table 5. Quantitative analysis results for individual stem cell cases. Regions positive for stem cells are represented in red and labeled as positive. Regions negative for stem cells are represented in black and labeled as negative. When no number is listed, the corresponding data point was unavailable.

Works Cited

- Alexianu, M.E., Kozovska, M. & Appel, S.H. (2001) Immune reactivity in a mouse model of familial ALS correlates with disease progression. *Neurology*, **57**, 1282-1289.
- Anderson PM. Genetic Aspects of Amyotrophic Lateral Sclerosis/Motor Neurone Disease. In: Shaw PJ, Strong MJ, editor. Motor Neuron Disorders. Vol. 28. Philadelphia: Butterworth Heinemann; 2003. pp. 207–208.
- Appel, S.H., Zhao, W., Beers, D.R. & Henkel, J.S. (2011) The microglial-motoneuron dialogue in ALS. *Acta Myol*, **30**, 4-8.
- Beers, D.R., Henkel, J.S., Xiao, Q., Zhao, W., Wang, J., Yen, A.A., Siklos, L., McKercher, S.R. & Appel, S.H. (2006) Wild-type microglia extend survival in PU.1 knockout mice with familial amyotrophic lateral sclerosis. *Proc Natl Acad Sci U S A*, **103**, 16021-16026.
- Beers, D.R., Zhao, W., Liao, B., Kano, O., Wang, J., Huang, A., Appel, S.H. & Henkel, J.S. (2011) Neuroinflammation modulates distinct regional and temporal clinical responses in ALS mice. *Brain Behav Immun*, **25**, 1025-1035.
- Boche, D., Perry, V.H. & Nicoll, J.A. (2013) Review: activation patterns of microglia and their identification in the human brain. *Neuropathol Appl Neurobiol*, **39**, 3-18.
- Brettschneider, J., Toledo, J.B., Van Deerlin, V.M., Elman, L., McCluskey, L., Lee, V.M. & Trojanowski, J.Q. (2012) Microglial activation correlates with disease progression and upper motor neuron clinical symptoms in amyotrophic lateral sclerosis. *PLoS One*, **7**, e39216.
- Butovsky, O., Jedrychowski, M.P., Cialic, R., Krasemann, S., Murugaiyan, G., Fanek, Z., Greco, D.J., Wu, P.M., Doykan, C.E., Kiner, O., Lawson, R.J., Frosch, M.P., Pochet, N., Fatimy, R.E., Krichevsky, A.M., Gygi, S.P., Lassmann, H., Berry, J., Cudkowicz, M.E. & Weiner, H.L. (2015) Targeting miR-155 restores abnormal microglia and attenuates disease in SOD1 mice. *Ann Neurol*, **77**, 75-99.
- Chen, S., Sayana, P., Zhang, X. & Le, W. (2013) Genetics of amyotrophic lateral sclerosis: an update. *Mol Neurodegener*, **8**, 28.
- Chio, A., Logroscino, G., Hardiman, O., Swingler, R., Mitchell, D., Beghi, E., Traynor, B.G. & Eural, C. (2009) Prognostic factors in ALS: A critical review. *Amyotroph Lateral Scler*, **10**, 310-323.
- Clement, A.M., Nguyen, M.D., Roberts, E.A., Garcia, M.L., Boillee, S., Rule, M., McMahon, A.P., Doucette, W., Siwek, D., Ferrante, R.J., Brown, R.H., Jr., Julien, J.P., Goldstein, L.S. & Cleveland, D.W. (2003) Wild-type nonneuronal cells extend survival of SOD1 mutant motor neurons in ALS mice. *Science*, **302**, 113-117.
- Colburn, R.W., DeLeo, J.A., Rickman, A.J., Yeager, M.P., Kwon, P. & Hickey, W.F. (1997) Dissociation of microglial activation and neuropathic pain behaviors following peripheral nerve injury in the rat. *J Neuroimmunol*, **79**, 163-175.
- Czaplinski, A., Yen, A.A., Simpson, E.P. & Appel, S.H. (2006) Slower disease progression and prolonged survival in contemporary patients with amyotrophic lateral sclerosis: is the natural history of amyotrophic lateral sclerosis changing? *Arch Neurol*, **63**, 1139-1143.
- Davalos, D., Grutzendler, J., Yang, G., Kim, J.V., Zuo, Y., Jung, S., Littman, D.R., Dustin, M.L. & Gan, W.B. (2005) ATP mediates rapid microglial response to local brain injury in vivo. *Nat Neurosci*, **8**, 752-758.
- de Carvalho, M., Matias, T., Coelho, F., Evangelista, T., Pinto, A. & Luis, M.L. (1996) Motor neuron disease presenting with respiratory failure. *J Neurol Sci*, **139 Suppl**, 117-122.

- Dewil, M., Van Den Bosch, L. & Robberecht, W. (2007) Microglia in amyotrophic lateral sclerosis. *Acta Neurol Belg*, **107**, 63-70.
- del Aguila, M.A., Longstreth, W.T., Jr., McGuire, V., Koepsell, T.D. & van Belle, G. (2003) Prognosis in amyotrophic lateral sclerosis: a population-based study. *Neurology*, **60**, 813-819.
- del Rio Hortega, P., *Microglia*, in *Cytology and Cellular Pathology of the Nervous System*, W. Penfield, Editor. 1932, Paul B. Hoeber: New York. p. 482-534
- Donnelly, D.J., Gensel, J.C., Ankeny, D.P., van Rooijen, N. & Popovich, P.G. (2009) An efficient and reproducible method for quantifying macrophages in different experimental models of central nervous system pathology. *J Neurosci Methods*, **181**, 36-44.
- Elliott, J.L. (2001) Cytokine upregulation in a murine model of familial amyotrophic lateral sclerosis. *Brain Res Mol Brain Res*, **95**, 172-178.
- Feldman, E.L., Boulis, N.M., Hur, J., Johe, K., Rutkove, S.B., Federici, T., Polak, M., Bordeau, J., Sakowski, S.A. & Glass, J.D. (2014) Intraspinal neural stem cell transplantation in amyotrophic lateral sclerosis: phase 1 trial outcomes. *Ann Neurol*, **75**, 363-373.
- Frakes, A.E., Ferraiuolo, L., Haidet-Phillips, A.M., Schmelzer, L., Braun, L., Miranda, C.J., Ladner, K.J., Bevan, A.K., Foust, K.D., Godbout, J.P., Popovich, P.G., Guttridge, D.C. & Kaspar, B.K. (2014) Microglia induce motor neuron death via the classical NF-kappaB pathway in amyotrophic lateral sclerosis. *Neuron*, **81**, 1009-1023.
- Ghatak, N.R., Campbell, W.W., Lippman, R.H. & Hadfield, M.G. (1986) Anterior horn changes of motor neuron disease associated with demyelinating radiculopathy. *J Neuropathol Exp Neurol*, **45**, 385-395.
- Glass, J.D., Hertzberg, V.S., Boulis, N.M., Riley, J., Federici, T., Polak, M., Bordeau, J., Fournier, C., Johe, K., Hazel, T., Cudkowicz, M., Atassi, N., Borges, L.F., Rutkove, S.B., Duell, J., Patil, P.G., Goutman, S.A. & Feldman, E.L. (2016) Transplantation of spinal cord-derived neural stem cells for ALS: Analysis of phase 1 and 2 trials. *Neurology*, **87**, 392-400.
- Glass, J.D., Boulis, N.M., Johe, K., Rutkove, S.B., Federici, T., Polak, M., Kelly, C. & Feldman, E.L. (2012) Lumbar intraspinal injection of neural stem cells in patients with amyotrophic lateral sclerosis: results of a phase I trial in 12 patients. *Stem Cells*, **30**, 1144-1151.
- Gordon, P.H., Cheng, B., Katz, I.B., Pinto, M., Hays, A.P., Mitsumoto, H. & Rowland, L.P. (2006) The natural history of primary lateral sclerosis. *Neurology*, **66**, 647-653.
- Gordon, S. & Martinez, F.O. (2010) Alternative activation of macrophages: mechanism and functions. *Immunity*, **32**, 593-604.
- Gurney, M.E., Pu, H., Chiu, A.Y., Dal Canto, M.C., Polchow, C.Y., Alexander, D.D., Caliendo, J., Hentati, A., Kwon, Y.W., Deng, H.X. & et al. (1994) Motor neuron degeneration in mice that express a human Cu,Zn superoxide dismutase mutation. *Science*, **264**, 1772-1775.
- Hampton, D.W., Anderson, J., Pryce, G., Irvine, K.A., Giovannoni, G., Fawcett, J.W., Compston, A., Franklin, R.J., Baker, D. & Chandran, S. (2008) An experimental model of secondary progressive multiple sclerosis that shows regional variation in gliosis, remyelination, axonal and neuronal loss. *J Neuroimmunol*, **201-202**, 200-211.
- Harraz, M.M., Marden, J.J., Zhou, W., Zhang, Y., Williams, A., Sharov, V.S., Nelson, K., Luo, M., Paulson, H., Schoneich, C. & Engelhardt, J.F. (2008) SOD1 mutations disrupt redox-sensitive Rac regulation of NADPH oxidase in a familial ALS model. *J Clin Invest*, **118**,

- 659-670.
- Harry, G.J. & Kraft, A.D. (2012) Microglia in the developing brain: a potential target with lifetime effects. *Neurotoxicology*, **33**, 191-206.
- Henkel, J.S., Beers, D.R., Zhao, W. & Appel, S.H. (2009) Microglia in ALS: the good, the bad, and the resting. *J Neuroimmune Pharmacol*, **4**, 389-398.
- Ito, D., Imai, Y., Ohsawa, K., Nakajima, K., Fukuuchi, Y. & Kohsaka, S. (1998) Microglia-specific localisation of a novel calcium binding protein, Iba1. *Brain Res Mol Brain Res*, **57**, 1-9.
- Kettenmann, H., Banati, R. & Walz, W. (1993) Electrophysiological behavior of microglia. *Glia*, **7**, 93-101.
- Kettenmann, H., Hanisch, U.K., Noda, M. & Verkhratsky, A. (2011) Physiology of microglia. *Physiol Rev*, **91**, 461-553.
- Komine, O. & Yamanaka, K. (2015) Neuroinflammation in motor neuron disease. *Nagoya J Med Sci*, **77**, 537-549.
- Lasiene, J. & Yamanaka, K. (2011) Glial cells in amyotrophic lateral sclerosis. *Neurol Res Int*, **2011**, 718987.
- Lawson, L.J., Perry, V.H., Dri, P. & Gordon, S. (1990) Heterogeneity in the distribution and morphology of microglia in the normal adult mouse brain. *Neuroscience*, **39**, 151-170.
- Liao, B., Zhao, W., Beers, D.R., Henkel, J.S. & Appel, S.H. (2012) Transformation from a neuroprotective to a neurotoxic microglial phenotype in a mouse model of ALS. *Exp Neurol*, **237**, 147-152.
- Louwerse, E.S., Visser, C.E., Bossuyt, P.M. & Weverling, G.J. (1997) Amyotrophic lateral sclerosis: mortality risk during the course of the disease and prognostic factors. The Netherlands ALS Consortium. *J Neurol Sci*, **152 Suppl 1**, S10-17.
- Manjaly, Z.R., Scott, K.M., Abhinav, K., Wijesekera, L., Ganesalingam, J., Goldstein, L.H., Janssen, A., Dougherty, A., Willey, E., Stanton, B.R., Turner, M.R., Ampong, M.A., Sakel, M., Orrell, R.W., Howard, R., Shaw, C.E., Leigh, P.N. & Al-Chalabi, A. (2010) The sex ratio in amyotrophic lateral sclerosis: A population based study. *Amyotroph Lateral Scler*, **11**, 439-442.
- Martinez, F.O., Helming, L. & Gordon, S. (2009) Alternative activation of macrophages: an immunologic functional perspective. *Annu Rev Immunol*, **27**, 451-483.
- McGuire, V., Longstreth, W.T., Jr., Koepsell, T.D. & van Belle, G. (1996) Incidence of amyotrophic lateral sclerosis in three counties in western Washington state. *Neurology*, **47**, 571-573.
- Moisse, K. & Strong, M.J. (2006) Innate immunity in amyotrophic lateral sclerosis. *Biochim Biophys Acta*, **1762**, 1083-1093.
- Nimmerjahn, A., Kirchhoff, F. & Helmchen, F. (2005) Resting microglial cells are highly dynamic surveillants of brain parenchyma in vivo. *Science*, **308**, 1314-1318.
- Papadimitriou, D., Le Verche, V., Jacquier, A., Ikiz, B., Przedborski, S. & Re, D.B. (2010) Inflammation in ALS and SMA: sorting out the good from the evil. *Neurobiol Dis*, **37**, 493-502.
- Pehar, M., Cassina, P., Vargas, M.R., Castellanos, R., Viera, L., Beckman, J.S., Estevez, A.G. & Barbeito, L. (2004) Astrocytic production of nerve growth factor in motor neuron apoptosis: implications for amyotrophic lateral sclerosis. *J Neurochem*, **89**, 464-473.
- Pocock, J.M. & Kettenmann, H. (2007) Neurotransmitter receptors on microglia. *Trends*

- Neurosci*, **30**, 527-535.
- Priller, J., Haas, C.A., Reddington, M. & Kreutzberg, G.W. (1995) Calcitonin gene-related peptide and ATP induce immediate early gene expression in cultured rat microglial cells. *Glia*, **15**, 447-457.
- Rothstein, J.D. (2009) Current hypotheses for the underlying biology of amyotrophic lateral sclerosis. *Ann Neurol*, **65 Suppl 1**, S3-9.
- Rosen, D.R. (1993) Mutations in Cu/Zn superoxide dismutase gene are associated with familial amyotrophic lateral sclerosis. *Nature*, **364**, 362.
- Tadesse, T., Gearing, M., Senitzer, D., Saxe, D., Brat, D.J., Bray, R., Gebel, H., Hill, C., Boulis, N., Riley, J., Feldman, E., Johe, K., Hazel, T., Polak, M., Bordeau, J., Federici, T. & Glass, J.D. (2014) Analysis of graft survival in a trial of stem cell transplant in ALS. *Ann Clin Transl Neurol*, **1**, 900-908.
- Takeuchi, H., Mizoguchi, H., Doi, Y., Jin, S., Noda, M., Liang, J., Li, H., Zhou, Y., Mori, R., Yasuoka, S., Li, E., Parajuli, B., Kawanokuchi, J., Sonobe, Y., Sato, J., Yamanaka, K., Sobue, G., Mizuno, T. & Suzumura, A. (2011) Blockade of gap junction hemichannel suppresses disease progression in mouse models of amyotrophic lateral sclerosis and Alzheimer's disease. *PLoS One*, **6**, e21108.
- Turner, M.R., Cagnin, A., Turkheimer, F.E., Miller, C.C., Shaw, C.E., Brooks, D.J., Leigh, P.N. & Banati, R.B. (2004) Evidence of widespread cerebral microglial activation in amyotrophic lateral sclerosis: an [11C](R)-PK11195 positron emission tomography study. *Neurobiol Dis*, **15**, 601-609.
- Vargas, M.R. & Johnson, J.A. (2010) Astrogliosis in amyotrophic lateral sclerosis: role and therapeutic potential of astrocytes. *Neurotherapeutics*, **7**, 471-481.
- Waltz, D.A., Sailor, L.Z. & Chapman, H.A. (1993) Cytokines induce urokinase-dependent adhesion of human myeloid cells. A regulatory role for plasminogen activator inhibitors. *J Clin Invest*, **91**, 1541-1552.
- Weydt, P., Yuen, E.C., Ransom, B.R. & Moller, T. (2004) Increased cytotoxic potential of microglia from ALS-transgenic mice. *Glia*, **48**, 179-182.
- Xu, L., Yan, J., Chen, D., Welsh, A.M., Hazel, T., Johe, K., Hatfield, G. & Koliatsos, V.E. (2006) Human neural stem cell grafts ameliorate motor neuron disease in SOD-1 transgenic rats. *Transplantation*, **82**, 865-875.
- Zarei, S., Carr, K., Reiley, L., Diaz, K., Guerra, O., Altamirano, P.F., Pagani, W., Lodin, D., Orozco, G. & Chinea, A. (2015) A comprehensive review of amyotrophic lateral sclerosis. *Surg Neurol Int*, **6**, 171.
- Zhao, W., Xie, W., Le, W., Beers, D.R., He, Y., Henkel, J.S., Simpson, E.P., Yen, A.A., Xiao, Q. & Appel, S.H. (2004) Activated microglia initiate motor neuron injury by a nitric oxide and glutamate-mediated mechanism. *J Neuropathol Exp Neurol*, **63**, 964-977.
- Zhao, Weihua., et al., "Immune-mediated Mechanisms in the Pathoprogession of Amyotrophic Lateral Sclerosis." *Journal of Neuroimmune Pharmacology : The Official Journal of the Society on NeuroImmune Pharmacology* (2013). U.S. National Library of Medicine, n.d. Web. 5 June 2015.